

JOURNÉES DE LA DIFFUSION

NEUTRONIQUE 2018

JUDIN 2018

14-16 MAI 2018

ROQUEBRUNE - GUR - ARGENG



UNIVERSITÉ
PARIS-EST CRÉTEIL
VAL DE MARNE



PROGRAM

	Monday 14th May		Tuesday 15th May		Wednesday 16th May
		8:30-9:15	SFN PhD Award <i>President: Charles Simon</i>		
		9:15-10:00	Winner's talk	9:15-10:00	Condensed Matter invited speaker: Arnaud Desmedt
		10:00-10:25	Break	10:00-10:25	Break
		10:25-11:10	Biology invited speaker: Guillaume Tresset	10:25-10:45	Evgeny Clementyev
				10:45-11:05	Thibault Charpentier
		11:10-11:30	Ekaterina Iashina	11:05-11:25	Afonso da Cunha Ferreira
		11:30-11:50	Guillaume Sudre	11:25-11:45	Monica Ceretti
		11:50-12:10	François Boué	11:45-12:00	Concluding remarks
12:00-14:00	Lunch	12:10-14:00	Lunch	12:00-14:00	Lunch
14:00-15:00	Welcome	14:00-14:45	Magnetism invited speaker: Romain Sibille		
15:00-15:45	Soft Matter invited speaker: Olivier Sandre	14:45-15:05	Evgenii Altynbaev		
		15:05-15:25	Françoise Damay		
15:45-16:05	Sandrine Lyonnard	15:25-15:45	Sylvain Petit		
16:05-16:25	Fabrice Cousin	15:45-16:05	Ketty Beauvois		
16:25-16:45	Nicolas Jouault	16:05-16:30	Break		
16:45-17:05	Jacques Jfestin	16:30-17:15	Instrumentation invited speaker: Jean-Marc Zanotti		
17:05-17:30	Break				
17:30 ...	ESS, ILL, LLB news	17:15-17:35	Martin Boehm		
		17:35-17:55	Frédéric Ott		
... 19:00		17:55 ...	Discussions Neutrons in the future <i>2FDN ENSA AG-SFN</i>		
19:00-19:30	CLIPs	...19:30			
19:30-21:00	Diner	19:30-21:00	Gala Diner		
21:00 ...	Posters	21:00 ...	Party		

GOFT MATTER

EGGION

SANS studies of polymer chains, “hybrid” core-shells, micelles and vesicles made of magnetic iron oxide nanoparticles, (co)polymers, polypeptides and phospholipids

Olivier Sandre^{1*}, Gauvin Hémery¹, Hélène Meheust¹, Etienne Grau¹, Henri Cramail¹, Elisabeth Garanger¹, Sébastien Lecommandoux¹, Annie Brûlet², Ralf Schweins³, Sarah MacEwan⁴, Ashutosh Chilkoti⁴, Thi Phuong Tuyen Dao¹, Fabio Fernandes⁵, Manuel Prieto⁵, Mériem Er-Rafik⁶, Marc Schmutz⁶, and Jean-François Le Meins¹

¹Laboratoire de Chimie des Polymères Organiques (LCPO), UMR5629 CNRS / Université de Bordeaux / Institut Polytechnique de Bordeaux, Pessac 33607 Cedex, France

²Laboratoire Léon Brillouin, UMR12 CNRS/CEA, CEA-Saclay, Gif-sur-Yvette 91191, France

³Institut Laue-Langevin (ILL) CS20156, 71 Avenue des Martyrs, 38042 Grenoble 9, France

⁴Department of Biomedical Engineering, Duke University, Durham, NC27708, USA

⁵Centro de Química-Física Molecular, Instituto Superior Técnico, Lisboa, Portugal

⁶Institut Charles Sadron (ICS) UPR 22 CNRS / Université de Strasbourg, Strasbourg, France

[*olivier.sandre@enscbp.fr](mailto:olivier.sandre@enscbp.fr)

This lecture will cover several soft matter colloidal systems where SANS brings useful information as non-perturbative method, some of them biology-oriented, of core-shell, micellar or vesicular structure, self-assembled from inorganic nanoparticles, polypeptides, or block copolymers and phospholipids. With perfectly defined sequence and chain length, recombinant peptides obtained by protein engineering allow investigating the structure-property relationships at a level of detail difficult to achieve with synthetic polymers. The temperature-triggered self-assembly of recombinant elastin-like block peptides (ELP) was studied by SANS for diblock ELPs^{1,2} and more recently for tri-block and gradient copolymers.³ On our side, we studied diblock ELP solutions below and above the critical micellar temperature (CMT) by multi-angle DLS and SANS. Below the CMT, the radius of gyration follows a power law *versus* molecular weight similar to Gaussian coils. Above CMT, attractive interactions between the more hydrophobic block of the ELP copolymers trigger the self-assembly into micelles. Continuing to raise temperature expels more and more water molecules out of the micelle core, the hydration level decreasing to just few D₂O per aminoacid, as estimated from the contrast in light and neutron scattering. These SANS studies highlight strong similarities between ELPs and synthetic copolymers: the standard Debye model of Gaussian chains enables fitting the scattering of ELP unimer chains and other systems. This is also the case for estolide polyesters which are bio-sourced polymers derived from natural oils. The thermal behavior is however opposite: unlike for ELPs where water switches from a Theta to a bad solvent, for these polyesters the solvent quality increases with temperature, as also assessed by intrinsic viscosity measurements. Besides self-assembled micelles, we studied the grafting of the diblock ELPs in the brush regime on iron oxide cores using a new “convergent” strategy,⁴ evidencing their response to application of an alternating magnetic field (AMF) by *in situ* DLS. SANS also gave us also information on the specific area in the case of multicore particles (nanoflowers),⁵ or on magnetic dispersions in crystallized waxes coated by silica shells that melt under an applied AMF.⁶ Other kinds of hybrid structures were studied by SANS, *i.e.* intimately mixed polymer/lipid vesicles based on poly(dimethyl siloxane) and poly(ethylene oxide) blocks of varying molar masses and architectures (*graft*, *triblock*), mixed with phospholipids (SOPC, DPPC...). Combining respective benefits of liposomes or polymersomes, Large Unilamellar Hybrid Vesicles (LUHVs) were studied at nanoscale by combining SANS, fluorescence spectroscopy and electron cryo-microscopy.⁷ A complete panorama of these LHUVs was obtained, ranging from wormlike hybrid micelles to either homogeneous or heterogeneous LHUVs, *i.e.* with membranes presenting lipid domains which SANS curves can be fitted by a holey vesicle form factor.⁸

¹ Garanger *et al.* *Macromol.* 2015, 48, 6617

² Hassouneh *et al.* *Macromol.* 2015, 48, 4183

³ MacEwan *et al.* *Biomac.* 2017, 18, 599

⁴ Hemery *et al.* *Mol. Syst. Des. Eng.* 2017, 2, 629

⁵ Hemery *et al.* *Inor. Chem.* 2017, 56, 8232

⁶ Baillot *et al.* *Part. Part. Syst. Charact.* 2017, 1700063

⁷ Tuyen Dao *et al.* *ACS Macro Lett.* 2015, 4, 182

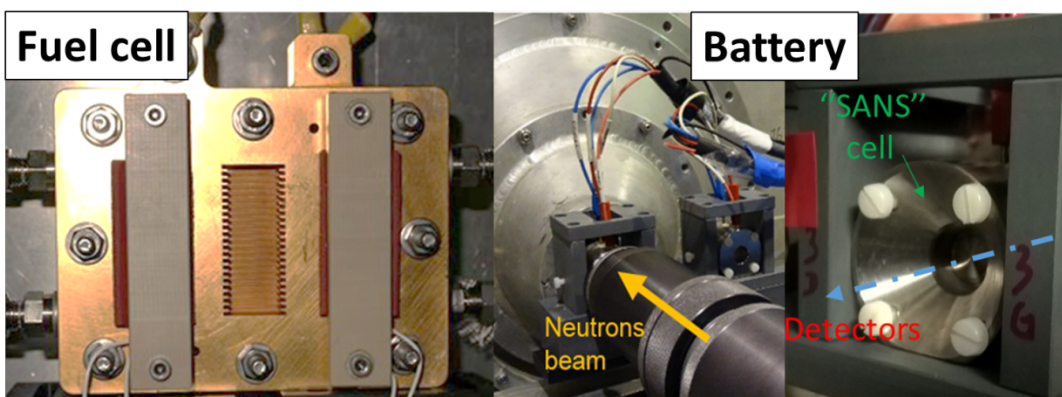
⁸ Tuyen Dao *et al.* *Langmuir* 2017, 33, 1705

Probing materials and devices for energy storage and conversion using neutron scattering

S. Lyonnard

CEA-INAC, SyMMES, Ionic Conducting Polymer Group, Grenoble, France.

Proton exchange membrane polymer fuel cells (PEMFC) and lithium ion batteries (LiB) are electrochemical devices used for conversion and energy storage applications. The structure and transport properties of nanomaterials employed as electrolytes or electrodes in these systems can be probed using different neutron scattering techniques, as SANS, QENS and imaging. The real-time evolution of the materials during operating can be also monitored *in situ*, using home-made neutron-transparent cells capable to operate in representative conditions (Figure). In this talk we will present the results of our most recent studies on proton conducting polymer membranes [1,2], water management in fuel cells [3], proton dynamics in fuel cells [4], and nanoscale morphology of silicon-based anodes for lithium-ion batteries [5]. In general, we will focus on highlighting the interest of neutrons to probe advanced materials and devices for energy.



- [1] H-D. Nguyen et al, ACS applied materials & interfaces, **2017**, 9 (2), pp 1671–1683
- [2] Q. Berrod et al, Sci. Rep. **2017** 7(1):8326. doi: 10.1038/s41598-017-08746-9
- [3] A. Morin et al, J. Electrochem. Soc. **2017**, 164 (2), 9-21
- [4] N. Martinez et al, J. Phys. Chem C **2018**, 122 (2), pp 1103–1108
- [4] S. Tardif et al, ACS Nano **2017** 11(11):11306-11316. doi: 10.1021/acsnano.7b05796

The « Extrapolation to zero concentration method »: a robust way for the determination of polymer conformation in nanocomposites

Anne-Sophie Robbes^{1,2}, Fabrice Cousin¹ and Jacques Jestin¹

¹ Laboratoire Léon Brillouin (CEA-CNRS), CEA Saclay, 91191 Gif-sur-Yvette Cedex

² Synchrotron Soleil, Saint-Aubin, BP 48, 91191 Gif-sur-Yvette Cedex

One of the main goal towards the understanding of the enhanced mechanical properties of nanocomposites, i.e. polymer melts filled with hard nanoparticles, is the determination of the conformation of the chains, whether they are free in the matrix or grafted on the nanofillers. To this aim, the only technique to access it is Small Angle Neutron Scattering (SANS) using labeling tricks based on mixture of hydrogenated and deuterated polymers that enable to cancel the contribution to the scattering of the filler. The method that is generally used is Zero Averaged Method (ZAC) that enables the determination of the chain form factor in a single measurement. Although very elegant, such ZAC method does not allow to check that the scattering of the filler is effectively matched. Moreover, it is only suitable to nanocomposite made of “naked” nanoparticles but not the ones where the fillers are grafted by the same chains as used in the matrix. To circumvent such drawbacks, we will show how to use an alternative and robust method known as “the extrapolation to zero concentration method”. Briefly, the idea is to use a system for which the neutron Scattering Length Density (SLD) of the filler is either similar to the SLD of the deuterated polymer or to the SLD of the hydrogenated one in order to match the scattering of the filler by the matrix. Then, several samples are made with various contents in hydrogenated polymers, which enables to decouple the contribution of the form factor and the structure factor within the chain scattering signal.

We will illustrate it by showing a series of experiments based on the same experimental model system made of polystyrene and magnetic nanoparticles of Fe_2O_3 that have the same SLD as deuterated PS where we probe various organizations of the nanofillers [1]: (i) homogeneous isotropic dispersion aggregates of naked nanoparticles [2]; (ii) chains of naked nanoparticles aligned over the whole sample [3]; (iii) perfect dispersion of grafted nanoparticles [4]; (iv) homogeneous isotropic dispersion of large aggregates of grafted nanoparticles [4]; (v) chains of large aggregates of grafted nanoparticles objects aligned over the whole sample [4]. We highlight small change of conformation of PS chains with respect to those of the pure melts: in case of naked particles, I.e. attractive interactions between fillers and polymer chains, the radius of gyration is swollen while it is reduced in the athermal case of grafted nanoparticles.

[1] A.-S. Robbes, F. Cousin *et al*, Macromolecules, 2018, DOI: 10.1021/acs.macromol.7b02318.

[2] A.-S. Robbes, J. Jestin *et al*, Macromolecules, 2010, 43(13), 5785–5796.

[3] A.-S. Robbes, J. Jestin *et al*, Macromolecules, 2011, 44(22), 8858–8865.

[4] A.-S. Robbes, F. Cousin *et al*, Macromolecules, 2012, 45, 9220–9231.

Unperturbed Polymer Chain Conformation in the Presence of Very Small Nanoparticles

N. Jouault¹, M.K. Crawford² and S.K. Kumar³

¹ Sorbonne Université, Laboratoire PHENIX, F-75005, Paris, France

² DuPont Central Research and Development, E400/5424, Wilmington, and Department of Physics and Astronomy, University of Delaware, USA

³ Department of Chemical Engineering, Columbia University, New York, USA

There has been a great deal of recent attention on the effects of nanoparticles (NPs) on polymer chain conformations in polymer nanocomposites (PNCs). In addition to its intrinsic fundamental interest, changes in polymer conformation may significantly influence the practically important mechanical properties of the PNCs. The foundational question of whether the presence of well-dispersed NPs changes the host polymer conformation, characterized by the radius of gyration R_g , has unfortunately been the source of considerable controversy. Here we focus on the case of PNCs containing very small NPs (VSNPs, diameters of 1-2 nm) where large chain expansions were observed for two different polymer-NP systems [1,2]. Small-Angle Neutron Scattering (SANS) measurements have been performed on PMMA mixed with weakly attractive 1.0 nm diameter polyhedral oligomeric silsesquioxane (POSS, Fig.1). Our results show no observable changes in the R_g , regardless of the PMMA molecular weight, the amount of residual solvent, or the POSS loading (from 0 to 20 % by volume). In retrospect, these results are not surprising since scaling arguments imply that chain size in the concentrated region of the phase diagram of a polymer solution is ideal and independent of the polymer volume fraction ϕ , and only as the semi-dilute region is entered with decreasing concentration does the chain size for a good solvent begin to scale as $\phi^{-1/2}$. For typical NP concentrations (less than 50 % v/v), PNCs are well within the concentrated polymer regions of their phase diagrams, where ideal chain conformations are observed for small molecule solvents. By combining the present results with previous results from literature, we conclude that NPs apparently have little effect on the polymer conformations, especially in typical PNCs that only incorporate moderate amounts of NPs.

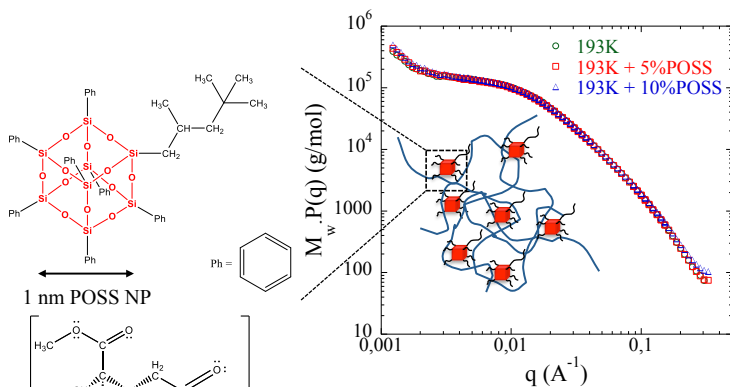


Figure 1: Schematic representation of the POSS molecule. SANS scattering intensities without and with (5% or 10 % v/v) POSS NPs.

[1] Nakatani, A. I.; Chen, W.; Schmidt, R. G.; Gordon, G. V.; Han, C. C., *Polymer*, 42 (2001) 3713-3722.

[2] Tuteja, A.; Duxbury, P. M.; Mackay, M. E., *PRL*, 100 (2008) 077801.

Organisation multi-échelle contrôlée de nanoparticules dans une matrice polymère semi-cristallin par cristallisation isotherme

Dan Zhao[†], Vianney Gimenez-Pinto[†], Andrew M. Jimenez[†], Jacques JESTIN^{§*}, Sanat K. Kumar[‡]

[†]Department of Chemical Engineering, Columbia University, New York, New York 10027, United States

[§]Laboratoire Léon Brillouin UMR12 CEA/CNRS, CEA Saclay 91191 Gif/Yvette Cedex France

[*jacques.jestin@cea.fr](mailto:jacques.jestin@cea.fr)

Mots-clés: Nanocomposites, Conformation, Nanoparticles dispersion, Scattering Methods.

Nous présentons une nouvelle méthode pour organiser hiérarchiquement des nanoparticules dans une matrice polymère semi-cristallin à différentes échelles caractéristiques (du nanomètre au micron) par le biais de la cristallisation isotherme du polymère. Le système expérimental consiste une matrice de Poly-oxyéthylène PEO ($M_w=100\text{kg/mol}$) au sein de laquelle sont dispersées des nanoparticules de silice ($R=14\text{nm}$, 3% vol.) greffées de chaînes de Polyméthacrylate de méthyle PMMA ($M_w=24\text{ kg/mol}$). Ce processus multi-échelle est piloté par la morphologie des cristaux à partir d'une situation où les particules sont initialement dispersée individuellement dans la matrice (i) une fraction des particules est incorporée dans le cristal et reste bien dispersée à l'échelle locale 10nm, (ii) une fraction des particules s'organisent en chaînes de particules anisotropes de part et d'autre de la lamelle cristalline à une échelle de taille supérieur 100 nm (iii) une fraction de particules forment des agrégats compacts entre les fibrilles cristallines à l'échelle du micron. La répartition des différentes fractions est contrôlée par la cinétique de cristallisation du polymère. A partir du bilan des forces répulsives et attractives entre la particule et le front de cristallisation, on définit un taux de croissance critique G_c typiquement compris entre 0.01 et 1micro-m/s pour une particule de rayon $R=10\text{nm}$ et ajustable en fonction de la température de cristallisation isotherme T_c . Comme illustré sur la Figure 1, lorsque le taux de croissance des cristaux est supérieur au taux de croissance critique ($T_c=52^\circ\text{C}$), l'ensemble des nanoparticules sont incorporées dans le cristal et dispersion initiale n'est pas modifiée. Au contraire, lorsque le taux de croissance est inférieur au taux de croissance critique ($T_c=58^\circ\text{C}$), les nanoparticules sont repoussées par le front de cristallisation, s'alignent le long des lamelles cristallines et s'agrègent entre les fibrilles. Le taux de croissance et la structure des cristaux sont déterminés par calorimétrie et microscopie optique. Les différentes organisations sont caractérisées par microscopie électronique et par une combinaison de mesures de diffusion de rayonnement aux petits angles (rayons x et neutrons) dont la modélisation permet de quantifier les fractions volumiques des différentes populations de particules (Figure 2). Ces résultats expérimentaux sont confirmés par des simulations numériques. Les structures obtenues ressemblent à des organisations naturelles telles que la nacre (alternance de couches organiques dans une phase inorganique) et lui confère comme pour cette dernière des propriétés mécaniques remarquables : un gain de près d'une décennie sur le seuil de percolation mécanique de renforcement (obtenu ici avec 1% vol. de particules alignées contre typiquement 10% vol. de particules dispersées de façon aléatoire) sans perte de module de résistance à la fracture. Cette approche nouvelle permet donc d'envisager des voies de fabrication de matériaux à base de polymères semi-cristallins à la fois renforcés mécaniquement, légers et résistants.

BIOLOGY

EGGION

Genome and polymer-filled icosahedral viruses

G. Tresset¹, M. Chevreuil¹, J. Chen¹, M. Tatou¹, C. Le Cœur², M. Zeghal¹, S. Combet², and L. Porcar³

¹ Laboratoire de Physique des Solides, CNRS, Université Paris-Saclay, Orsay, France

² Laboratoire Léon Brillouin, CEA, CNRS, Université Paris-Saclay, Gif-sur-Yvette, France

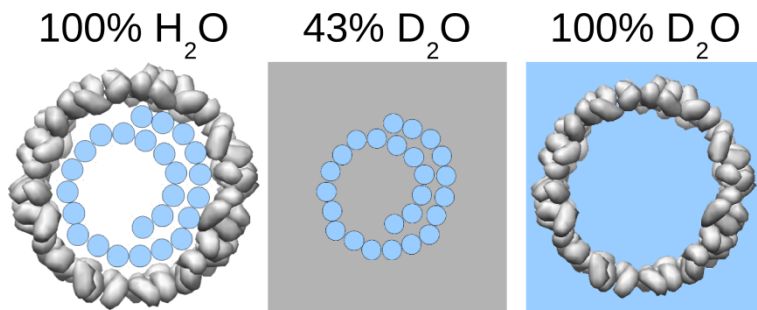
³ Institut Laue Langevin, Grenoble, France

The simplest icosahedral viruses can be viewed as nanometer-scaled protein shells called capsids encasing the genome in the form of nucleic acids. The cowpea chlorotic mottle virus (CCMV) is a nonenveloped single-stranded (ss)RNA plant virus, whose capsid (28 nm in diameter) is made up of 90 dimeric, chemically identical subunits arrayed onto an icosahedral lattice. Its multipartite genome consists of four ssRNA segments distributed in three indistinguishable particles in such a way that all particles package more or less the same mass of RNA, i.e., about 2,800 nucleotides. The virus self-assembles in its host cell and therefore captures the required segments of its genome with a remarkable selectivity. Whether such a level of selectivity is due to intricate molecular recognitions or to nonspecific interactions between genome and capsid is a much-debated question.

We showed that the thermal dissociation of CCMV virions proceeds through a two-dimensional first-order phase transition and the melting temperature could be related to the interaction energies between viral components via a mean field theory [1]. By using the contrast variation method in small-angle neutron scattering (SANS), we observed a slight shrinkage (~ 2 nm for the radius) of the genome-filled capsid upon an increase of temperature, prior to dissociation. This counterintuitive result can be ascribed to an enhanced hydrophobic interaction between subunits due to the increased temperature.

CCMV virions can be assembled *in vitro* from purified subunits and genome. We observed that the subunit-subunit and subunit-genome can be tuned via the pH and the ionic strength respectively. By contrast-matching the genome at neutral pH, we measured by SANS that no subunit was bound on the genome at high ionic strength (0.5 M), while 75 ± 31 subunits were bound on each genome segment at low ionic strength (0.1 M). Upon lowering the pH, we obtained particles comprising about 90 subunits, structurally identical to native virions.

Deuterated poly(styrene sulfonic acid) (d-PSS) with various molecular weight was packaged into viral capsids in order to assess the selectivity of subunits. The contrast variation method in SANS allowed us to accurately estimate the mean mass of packaged polymer $\langle M_p \rangle$ and that of the surrounding capsid $\langle M_{cap} \rangle$. Remarkably, the mass ratio $\langle M_p \rangle / \langle M_{cap} \rangle$ was invariant for molecular weights of polymer spanning more than two orders of magnitude [2]. Capsids either packaged several chains simultaneously or selectively retained the shortest chains that could fit the capsid interior. These data are in qualitative agreement with theoretical predictions based on free energy minimization and emphasize the importance of subunit self-energy. These findings suggest a nonspecific origin for the genome selectivity, at least for certain viral systems.



[1] J. Chen, M. Chevreuil, S. Combet, Y. Lansac, G. Tresset, J. Phys.: Condens. Matter, 29 (2017) 474001.

[2] G. Tresset, M. Tatou, C. Le Cœur, M. Zeghal, V. Bailleux, A. Lecchi, K. Brach, M. Klekotko, L. Porcar, Phys. Rev. Lett., 113 (2014) 128305.

Logarithmic fractal structure of the large-scale chromatin organization in the nuclei of the HeLa cell

E. G. Iashina^{1,2}, M. V. Filatov², R. A. Pantina², E. Y. Varfolomeeva², W. G. Bouwman³, C. P. Duif³, D. Honecker⁴, V. Pipich⁵ and S. V. Grigoriev^{1,2}

¹*Saint Petersburg State University, Ulyanovskaya 1, Saint Petersburg, 198504, Russia*

²*Petersburg Nuclear Physics Institute NRC "Kurchatov institute", Gatchina, St. Petersburg, 188300, Russia*

³*Delft University of Technology, Mekelweg 15, 2629 JB Delft, The Netherlands*

⁴*Institut Laue Langevin, F-38042 Cedex 9, Grenoble, France*

⁵*Heinz Maier-Leibnitz Zentrum, Lichtenbergstrasse 1, 85747 Garching, Germany*

The majority of eukaryotic cells spend most of their time in interphase. Interphase is the metabolic phase of cells, in which cells obtain nutrients and metabolize them, grow, read their DNA and synthesize proteins. Cells should do all these functions in a short time (nano or micro seconds). This fact requires very quick unpacking of DNA and finding a specific gene site, in order to read the genetic information. To achieve the extreme density of the DNA packing and high accessibility of enzymes to specific gene site nature uses the hierarchical principle of the structural organization. However, the question of how a meter-long DNA strand is packed into a micron nucleus is not completely resolved.

Using Small Angle Neutron Scattering and Spin-Echo Small Angle Neutron Scattering methods we have shown that the HeLa nucleus has the two-scale fractal structure of the chromatin organization: volume fractal structure on nanometer scales and logarithmic fractal structure on micron scales. Previously, we had proven the existence of the logarithmic fractal structure in the large scale organization in chicken erythrocyte nuclei [1]. Apparently, such structure is characteristic for interphase nuclei. We point out the difference between scattering patterns from the chicken erythrocyte and HeLa nuclei. Moreover the ability of HeLa nuclei to interpenetrate into each other upon agglomeration process was found and explained in this study.

[1] E. G. Iashina, E. V. Velichko, M. V. Filatov, W. G. Bouwman, C. P. Duif, A. Brulet, S. V. Grigoriev, Physical Review E vol. 96 N. 1 (2017).

Chitosan supported films: physicochemical characterizations and biological responses

M. Diallo¹, J. Tréguier², S. Trombotto¹, A. Montembault¹, O. Théodoly³, T. Mignot², L. David¹, T. Delair¹, G. Sudre^{1*}

¹ Ingénierie des Matériaux Polymères, CNRS-Université Claude Bernard Lyon 1, UMR 5223, 15 bd. A. Latarjet, 69100 Villeurbanne, France.

² Laboratoire de Chimie Bactérienne, CNRS-Aix Marseille University, UMR 7283, 31 Ch. J. Aiguier, 13009 Marseille, France.

³ Adhesion and Inflammation Laboratory, INSERM-CNRS-Aix Marseille University, UMR 7333, 163 av. de Luminy, 13009 Marseille, France.

Chitosan is a copolymer belonging to the class of polysaccharides. It is obtained by partial deacetylation of chitin, which is generally extracted from shrimp shells or squid pens. Chitosan is composed of D-glucosamine and N-acetyl-D-glucosamine units linked by β (1→4) glycosidic bonds (Fig. 1). [1]

Because of its biocompatibility, biodegradability and non-toxicity, this polysaccharide has received considerable attention for biomedical applications, *e.g.* for the preparation and the formulation of biologically compatible *in vivo* and *ex vivo* materials. [2] A recent study has shown that surfaces covered with chitosan can modulate bacteria adhesion, [3] from allowing the immobilization of bacteria (Fig. 2) without altering their reproduction, to being antibacterial. These variations depend on the molecular parameters of chitosan, and the control of the biological response could be used for the engineering of implant surfaces or the development of new devices for bacterial studies.

The aim of this work is to evaluate the physicochemical properties (thickness, wetting, surface energy, film morphology, swelling) and the biological responses of various surfaces modified with different chitosans. To this end, we have prepared a library of chitosans of various molar mass and DA, which have been dissolved in mild acidic conditions to form thin solid films by spin-coating. We will briefly discuss the wetting results and describe the swelling determined by neutron reflectivity of chitosan submicronic films as a function of DA (see Fig. 3) and of pH. We will then present some biological results to illustrate the difficult correlation between the physicochemical properties of chitosan films to the adhesion response of bacteria.

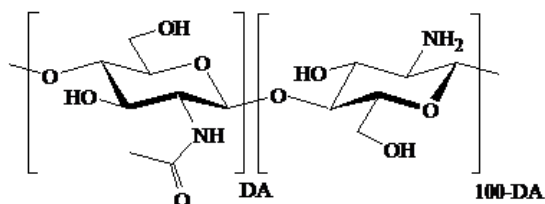


Figure 1: Chemical structure of chitosan.

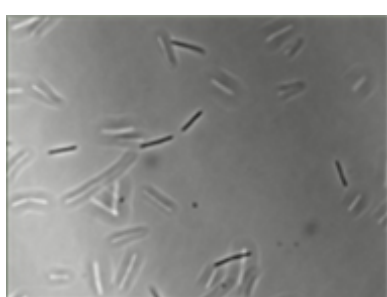


Figure 2: *E. Coli* adhesion on chitosan.

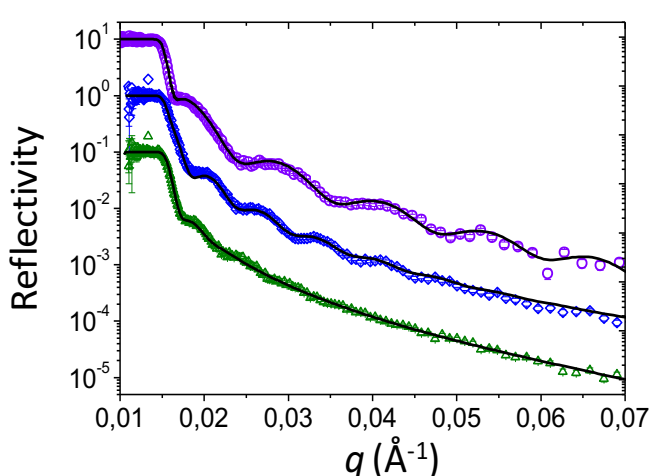


Figure 3: Reflectivity curves of chitosan films (dry thickness of about 250 Å) of various DA, swollen in D₂O at pH 7.1. From top to bottom: DA 1%, DA 9% and DA 14%.

[1] P. K. Dutta, J. Dutta, & V. S. Tripathi. Journal of Scientific and Industrial Research, 63 (2004) 20-31.

[2] C. Peniche, W. Argüelles-Monal, H. Peniche, & N. Acosta. Macromolecular Bioscience, 3 (2003) 511–520.

[3] L. M. Faure1, J.B. Fiche, L. Espinosa1, et al. Nature, 539 (2016) 530-535.

Monitoring food structure in plant protein solutions and gels during digestion

J. Pasquier^{1,2}, A. Boire⁴, F. Jamme², J. Perez², E. Lutton³, F. Boué^{1,3}, A. Brûlet¹

¹*Laboratoire Léon Brillouin, CEA-Saclay, F-91191 Gif-sur-Yvette, France*

²*Synchrotron SOLEIL, F-91192 Gif-sur-Yvette, France*

³*Génie et Microbiologie des Procédés Alimentaires, UMR0782 INRA - AgroParisTech, F-78850 Thiverval-Grignon, France*

⁴*Biopolymères, Interactions Assemblages, UR1268, INRA, F-44316 Nantes, France*

Leaning on experimental evidences that nutritional quality of food not only depends on its molecular composition but also on its structure, several measurements have been conducted on kinetics of dairy food matrices (milks and gels) during in vitro digestion through UV fluorescence imaging and SAXS (DISCO and SWING beam lines respectively at Synchrotron SOLEIL). SANS has also been used at LLB (PAXY, TPA) in order to study mixtures of proteins dairy gels with fat (from whole milk) by the way of contrast variation.

Through Jade Pasquier's PhD (LLB-SOLEIL-INRA), we have completed these studies and introduced new food models, plant proteins solutions/gels coming from rapeseed, which are part of the Global Food Security challenge highlighting the sustainable agriculture to fight against malnutrition: <http://www.globalfoodsecurityconference.com/>. In order to do this, two rapeseed storage proteins have been extracted and purified, i.e. napin and cruciferin, in collaboration with INRA-BIA. First experiments with same imaging and diffusion techniques have been led on in vitro digestion of these rapeseed proteins in solutions or in networks after thermally induced gelation, each of them at high alkaline pH (i.e. 11). Now, we aim to monitor their degradation kinetics at different pH, from 7 to 11, with an in-depth study of intestinal phase and finally in interaction with fat in a mixed food system.

MAGNETIC SIGN

SEGSSION

Signatures of quantumness in rare-earth pyrochlore oxides

Romain Sibille

Laboratory for Neutron Scattering and Imaging, Paul Scherrer Institut, 5232 Villigen PSI, Switzerland

Magnetic systems with competing interactions often adopt exotic ground states, which can be relevant to study new physics in quantum matter [1]. A recurrent ingredient to stabilize such phases is geometrical frustration, such as in pyrochlore oxides where rare-earth magnetic moments decorate a lattice of corner-sharing tetrahedra. An unusual spin liquid appears for example in the pyrochlore $\text{Ho}_2\text{Ti}_2\text{O}_7$, which features a classical ‘spin ice’ short-range correlated state [2,3]. A local constraint – the 2-in-2-out ‘ice rule’ acting on each tetrahedron – leads to a manifold of degenerate ground states in which the spin correlations give rise to emergent magnetostatics [4]. Spin flips violating the ice rule generate magnetic monopole excitations [5], a mobile magnetic charge regarded as a quasiparticle carrying half of the dipole moment. A quantum analogue of the spin ice state is predicted to be a special type of quantum spin liquid formed through the coherent superposition of spin ice configurations [6,7]. Remarkably, the low-energy physics of this *quantum spin ice* state is predicted to be a lattice analogue of quantum electrodynamics.

In $\text{Pr}_2\text{Hf}_2\text{O}_7$, the single-ion ground state doublet [10] has a dipole Ising-like moment of $\sim 2.4 \mu_B$, and electric quadrupoles that formally allow quantum tunneling between the in and out states of the dipole [11]. A correlated ground state with indications of spin ice correlations forms below 0.5 K [10]. Neutron scattering experiments demonstrate that the experimental structure factor has pinch points – a signature of a classical spin ice – that are partially suppressed, as expected in the presence of quantum dynamics [12]. Moreover, a continuum of magnetic excitations is observed in inelastic neutron scattering, which relates to the monopoles of spin ices that become quantum-coherent fractionalized excitations – akin to the spinons found for instance in quantum spin chains. Taken together, these two signatures strongly suggest that the low-energy physics of $\text{Pr}_2\text{Hf}_2\text{O}_7$ can be described by emergent quantum electrodynamics.

In $\text{Tb}_2\text{Hf}_2\text{O}_7$, neutron scattering experiments also provide strong arguments for the realization of a quantum spin liquid at low temperature [13]. However, the microscopic mechanism that brings quantum fluctuations into play is probably different here. Indeed, the detailed study of this material demonstrates that disorder can play a crucial role in preventing long-range magnetic order. This observation relates to a theoretical model of disorder-induced quantum fluctuations due to quenched random transverse fields acting on non-Kramers rare-earth ions [14].

- [1] Balents, L. *Nature* **464**, 199 (2010).
- [2] Bramwell, S. T. et al. *Phys. Rev. Lett.* **87**, 047205 (2001).
- [3] Castelnovo, C., Moessner, R. & Sondhi, S. L. *Annu. Rev. Condens. Matter Phys.* **3**, 35–55 (2012).
- [4] Fennell, T. et al. *Science* **326**, 415 (2009).
- [5] Castelnovo, C., Moessner, R. & Sondhi, S. L. *Nature* **451**, 42–45 (2008).
- [6] Hermele, M., Fisher, M. P. A. & Balents, L. *Phys. Rev. B* **69**, 064404 (2004).
- [7] Gingras, M. J. P. & McClarty, P. A. *Rep. Prog. Phys.* **77**, 056501 (2014).
- [8] Curnoe, S. H. *Phys. Rev. B* **78**, 094418 (2008).
- [9] Ross, K. A., Savary, L., Gaulin, B. D. & Balents, L. *Phys. Rev. X* **1**, 021002 (2011).
- [10] Sibille, R. et al. *Phys. Rev. B* **94**, 024436 (2016).
- [11] Onoda, S. & Tanaka, Y. *Phys. Rev. Lett.* **105**, 047201 (2010).
- [12] Sibille, R. et al. *Nature Physics* <http://dx.doi.org/10.1038/s41567-018-0116-x> (2018).
- [13] Sibille, R. et al. *Nature Commun.* **8**:892 (2017).
- [14] Savary, L. & Balents, L. *Phys. Rev. Lett.* **118**, 087203 (2017).

Evolution of the magnetic structure of $Mn_{1-x}Fe_xGe$ with $x < 0.35$ under external magnetic field

E. V. Altynbaev^{1,2,3}, K. A. Pschenichnyi^{1,2,3}, A. Heinemann⁴, G. Chaboussant⁵, N. Martin⁵,
A. Tsvyashchenko³, S. Grigoriev^{1,2,3}

¹ Petersburg Nuclear Physics Institute, Gatchina, 188300 St-Petersburg, Russia

² Faculty of Physics, Saint-Petersburg State University, 198504 Saint Petersburg, Russia

³ Institute for High Pressure Physics, 142190, Troitsk, Moscow Region, Russia.

⁴ Helmholtz Zentrum Geesthacht, 21502 Geesthacht, Germany

⁵ Laboratoire Leon Brillouin, CEA Saclay, 91191 Gif-sur-Yvette Cedex, France

We have grown $Mn_{1-x}Fe_xGe$ compounds with $x = 0.0, 0.3$ and 0.35 . These compounds can be synthesized under high pressure only [1]. All samples have been tested with the x-ray diffraction and show $B20$ type structure without any other phases. It is well known that the magnetic system of $Mn_{1-x}Fe_xGe$ $B20$ -type solid solutions with $x < 0.4$ orders into helical structure with a wave vector $k \approx 2 \text{ nm}^{-1}$ at low temperatures [2, 3]. The temperature evolution of the magnetic structure of $Mn_{1-x}Fe_xGe$ with $x < 0.4$ was already studied using small angle neutron scattering (SANS). Two quantum phase transitions at $x_{C1} \approx 0.25$ and $x_{C2} \approx 0.4$ have been found which system undergoes with increase of x [4]. Here we present comprehensive SANS measurements of the evolution of the magnetic structure of $Mn_{1-x}Fe_xGe$ (with $x = 0.0, 0.3$ and 0.35) under magnetic field. As the result the (H-T) phase diagrammes have been plotted for each compound. The critical temperatures T_N , T_h and T_{SR} found earlier for $Mn_{1-x}Fe_xGe$ compounds ($x < 0.4$) [3, 4] are better specified under applied field. The skyrmion lattice (A-phase) has been found for the $Mn_{1-x}Fe_xGe$ compounds with $x = 0.3$ and 0.35 , but it has not been detected for pure MnGe compound in the temperature range $90 \text{ K} < T < 200 \text{ K}$ and up to field $H = 10 \text{ T}$.

We suggest that the effective Ruderman-Kittel-Kasuya-Yosida interaction is the fundamental interaction resulting in the helical structure in MnGe. The increase of x modifies and (highly probable) destabilizes the effective RKKY interaction within the Heisenberg model of magnetism. The Dzyaloshinskii-Moriya interaction can be considered as an instrument for destabilization of the helical structure upon increase of x and serves as the main reason for the appearance of the skyrmion lattice (A-phase) in $Mn_{1-x}Fe_xGe$ solid solutions with $x > x_{C1} \approx 0.25$.

Authors thank for support the Russian Scientific Foundation (Grant No 17-12-01050).

- [1] A. V. Tsvyashchenko, J. Less-Common Met. 99, (1984) L9.
- [2] S.V. Grigoriev, et al., Phys. Rev. Lett., **110**, (2013) 207201.
- [3] E.V. Altynbaev, et al., Phys. Rev. B, **90**, (2014) 174420.
- [4] E.V. Altynbaev, et al., Phys. Rev. B, **94**, (2016) 174403.

Coupling magnetic sublattices in heterometallic ludwigite $\text{Fe}_{3-x}\text{Mn}_x\text{BO}_5$

F. Damay¹, L.Chaix¹, F. Lainé², A. Maignan², A. Guesdon², P. Beran³, F. Fauth⁴, J. Sotmann², L. Nataf⁴, S. Petit¹, and C. Martin²

¹ Laboratoire Léon Brillouin, CEA-CNRS UMR 12, 91191 GIF-SUR-YVETTE CEDEX, France

² Laboratoire CRISMAT, CNRS UMR 6508, 6 bd Maréchal Juin, 14050 CAEN CEDEX, France

³ Nuclear Physics Institute, Academy of Sciences of the Czech Republic, 25068 Rez near Prague, Czech Republic

⁴ Synchrotron Soleil, Saint-Aubin BP 48, 91192 GIF-sur-YVETTE Cedex, France

⁵ Synchrotron Alba, Carretera BP 1413, 08290 Cerdanyola del Vallès, BARCELONA, Spain

Ludwigite oxyborates $\text{M}_2\text{M}'\text{BO}_5$, where M and M' are divalent and trivalent 3d metal ions, respectively, have an intriguing orthorhombic crystal structure made of interconnected low dimensional units in the form of three-leg (3LL) ladders, 3LL1 and 3LL2 [1] (Figure 1).

The existence of two crystallographically distinct sublattices is not anodyne : in Fe_3BO_5 , Mössbauer and X-ray diffraction studies at room temperature have evidenced that Fe^{3+} species occupy preferentially 3LL1, while 3LL2 is occupied by Fe^{2+} [2]. In addition, a charge ordering transition has also been observed at $T_{\text{CO}} = 283$ K [1], [4], resulting from the ordering on 3LL1 of the extra itinerant electron within each Fe^{3+} triad. This also impacts the magnetic properties : according to neutron diffraction results, 3LL1 and 3LL2 magnetically order, but independently, at $T_{\text{N}1} = 112$ K and $T_{\text{N}2} = 70$ K, respectively, with orthogonal propagation vectors.

In the presented work, the isostructural system $\text{Fe}_{3-x}\text{Mn}_x\text{BO}_5$ has been studied by electron microscopy, neutron scattering, and Mn and Fe K-edge X-ray absorption, combined with physical properties measurements. . A decrease of both T_{N} 's, more pronounced for $T_{\text{N}2}$, along with a reduced ordered moment, is observed with increasing x, up to x = 1. For x = 1, only short-range magnetic ordering is observed on 3LL2, leading to a superparamagnetic ac susceptibility response [3], in agreement with the preferred substitution of Mn^{2+} on 3LL2. Surprisingly, however, for x = 1.5, 3D long-range ordering below $T_{\text{N}} = 100$ K is observed, which couples both 3LLs within a new collinear $\mathbf{k} = 0$ structure, without any sign of magnetic disorder.

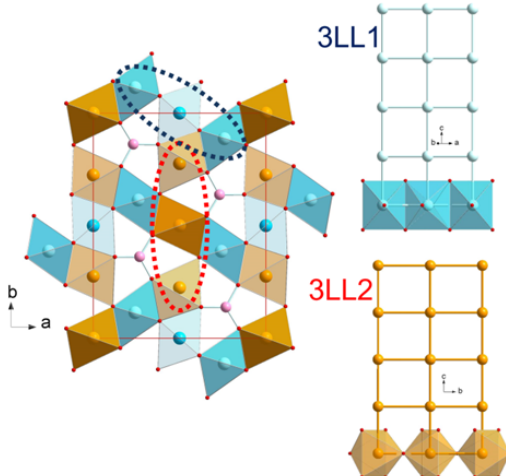


Figure 1 : Ludwigite crystal structure and its two square ladders sublattices.

- [1] M. MIR et al., Phys. Rev. Lett. 87, 147201 (2001) ; P. BORDET and E. SUARD, Phys. Rev. B 79, 144408 (2009).
- [2] A. P. DOUVALIS, et al., J. Phys. Cond. Matter 14, PII S0953 (2002).
- [3] A. MAIGNAN et al., J. Solid State Chem. 246, 209 (2017).

Effets quantiques dans les systèmes magnétiques frustrés de type «pyrochlore»

Sylvain Petit¹, Elsa Lhotel², Julien Robert²

¹ LLB, CEA Saclay, F-91191 Gif-sur-Yvette

² Institut Néel, F-38000 Grenoble

La frustration magnétique, c'est à dire l'incapacité d'un système à satisfaire simultanément l'ensemble de ses interactions, fait l'objet de nombreuses recherches en physique de la matière condensée. Ce phénomène, qui peut être lié à la topologie du réseau cristallin ou aux compétitions entre interactions, constitue la source de nouveaux états exotiques de la matière, dont la description va au-delà des modèles classiques. Les «glaces de spin» et leurs analogues quantiques, constituent un exemple emblématique de cette physique. La structure cristallographique de ces matériaux est basée sur un réseau de type «pyrochlore», formé d'un ensemble de tétraèdres connectés par leurs sommets, chaque nœud étant occupé par un ion de terre rare magnétique (Tb, Dy, Ho, Pr, etc.). Dans ces composés, les orbitales électroniques pertinentes ont une forme d'aiguille très fine, allongée en direction du centre de chaque tétraèdre. Le moment magnétique de chaque ion ne peut alors pointer que vers l'intérieur ou vers l'extérieur d'un tétraèdre, à l'instar des états $\downarrow\uparrow\downarrow\uparrow$ d'une variable Ising. L'état fondamental classique d'un tel système est très particulier car infiniment dégénéré. En effet, la seule prescription pour le construire est de suivre une règle locale qui stipule que chaque tétraèdre doit comporter deux spins «in» qui pointent vers l'intérieur et deux spins «out» qui pointent vers l'extérieur. Ces dernières années, les physiciens théoriciens ont proposé une vision nouvelle du problème, remarquant que la règle «two in-two out» est en fait analogue à la loi de conservation d'un flux magnétique fictif $\text{div } \mathbf{B}=0$ en électromagnétisme [1]. L'analogie est complète dès lors qu'on incorpore les fluctuations quantiques. En effet, les fluctuations du champ magnétique fictif B , créent en vertu de la loi de l'induction $\text{rot } \mathbf{E} = dB/dt$ un champ électrique «émergent» E . Selon les prédictions théoriques, une glace de spin quantique devrait comporter un spectre d'excitation particulier caractérisé par un mode analogue au photon de l'électromagnétisme.

A l'aide d'exemples tirés de la littérature, nous souhaitons montrer dans cet exposé qu'en dépit de nombreux travaux, les expériences réalisées jusqu'à aujourd'hui dans cette famille de composés n'ont pas encore permis de mettre en évidence cette dynamique particulière, à l'exception possible de $\text{Pr}_2\text{Hf}_2\text{O}_7$. Toutefois, l'influence des effets quantiques a très clairement été observée, mettant en lumière une très grande richesse de comportements. Nous discuterons en particulier le cas de $\text{Tb}_2\text{Ti}_2\text{O}_7$, l'influence des défauts dans $\text{Pr}_2\text{Zr}_2\text{O}_7$, la fragmentation magnétique dans $\text{Nd}_2\text{Zr}_2\text{O}_7$, ainsi que, au-delà de la physique propre aux spins Ising, l'ordre par le désordre dans $\text{Er}_2\text{Ti}_2\text{O}_7$ et la compétition d'interactions dans $\text{Yb}_2\text{Ti}_2\text{O}_7$.

[1] Quantum spin ice: a search for gapless quantum spin liquids in pyrochlore magnets, M.J.P. Gingras and P.A. McClarty, Rep Prog Phys 77 (2017) 056501.

Magnetic interactions in the frustrated pentagonal compound $\text{Bi}_2\text{Fe}_4\text{O}_9$

K. Beauvois¹, V. Simonet², E. Ressouche¹, S. Petit³, M. Gospodinov⁴ and V. Skumryev⁵

¹ CEA, INAC/SPSMS-MDN, Grenoble, France

² Institut Néel-CNRS, Grenoble, France

³ CEA-CNRS, LLB Saclay, France

⁴ Institute of Solid State Physics, Bulgarian Academy of Sciences, Bulgaria

⁵ Universitat Autònoma de Barcelona, Spain

The Fe^{3+} ions in $\text{Bi}_2\text{Fe}_4\text{O}_9$ materialize the first analogue of a magnetic pentagonal lattice [1]. The unit cell contains two different sites of four iron atoms each, which have different connectivities with the other irons (three or four neighbours for Fe_1 and Fe_2 respectively), and that form a lattice of pentagons. Because of its odd number of bonds per elemental brick, this lattice is prone to geometric frustration. The compound magnetically orders around 240 K: the resulting spin configuration on the two sites is the same, i.e. two orthogonal pairs of antiferromagnetic spins in a plane, with a global rotation between the two sites Fe_1 and Fe_2 . This peculiar magnetic structure, which is the result of the complex connectivity, has opened new perspectives in the field of magnetic frustration.

Here, we present the work in progress concerning the understanding and the consequences of the peculiar magnetic interactions in this original system. The magnetic excitations have been investigated by inelastic neutron scattering using thermal neutron triple axis spectrometers at the LLB and the ILL. The confrontation of the experimental results with spinwave calculations shows that there is a hierarchy of the interactions between the iron sites in the lattice and suggest that this system can be alternatively understood as a frustrated lattice of classical spin dimers. This transforms to a paramagnetic state of classical dimers above the Néel temperature as suggested by preliminary magnetization distribution maps measured at ILL using polarized neutrons under an applied magnetic field.

Our new experimental results on $\text{Bi}_2\text{Fe}_4\text{O}_9$ open interesting perspectives in the field of frustrated pentagonal lattices.

[1] E. Ressouche, V. Simonet, B. Canals, M. Gospodinov, V. Skumryev, Phys. Rev. Lett. 103, 267204 (2009).

INSTRUMENTATION

GEGGION

**IN6-SHARP: towards a new cold neutron spectrometer at ILL.
Illustration of the potentialities of QENS to probe the dynamics of Ionic liquids in bulk and under
1D nanometric confinement.**

F. Ferdeghini¹, Q. Berrod¹, P. Judeinstein¹, J. Dijon², J.-M. Zanotti¹

¹. Laboratoire Léon Brillouin (CEA-CNRS), Université Paris-Saclay, 91191 Gif-sur-Yvette, France

² CEA/LITEN/DTNM, 38054 Grenoble, France

Following the [agreement to strengthen the Franco-Swedish cooperation in the field of neutron scattering](#), the Laboratoire Léon Brillouin ([LLB](#)) is involved in the construction of an inelastic time-of-flight spectrometer. After the announcement of the Orphée reactor shutdown in 2020, the project originally planned at Saclay has been transferred to the Laue Langevin Institute ([ILL](#)). This renaissance takes the form of an A type [CRG](#) contract concluded on September 29th 2017 between the [DRF](#) of the CEA, the [INP](#) of the CNRS, and the [ILL](#). This new project [SHARP](#) (Spectromètre Hybride Alpes Région Parisienne) consists of a complete rebuilding of the [IN6](#) secondary spectrometer: sample environment, time-of-flight chamber and detection. This seminar will start by an update on the project.

We will then illustrate the potentialities of Quasi-Elastic Neutron Scattering (QENS) in the study of Ionic liquids (ILs). ILs are pure solutions of charged organic molecules with no solvent. These molecular electrolytes show a property original for a pure liquid: they self-organize in nanometric fluctuating aggregates [1]. When probed at the macroscopic scale, ILs behave as highly dissociated (*i.e.* strong) electrolytes [2] while, at the molecular scale, they show clear characteristics of weak ionic solutions [3]. In this talk, we report a multi-scale analysis that sheds new light on these apparently at odd behaviors [4,5].

Due to their remarkable chemical and electrochemical stability, ILs have been identified as prime candidates electrolytes for the development of new safe and sustainable energy storage systems. We show [6] a noticeable enhancement (by a factor 3) of the transport properties of a neat IL under CNT (Carbon NanoTube) confinement in a 1D situation. Such CNT membranes are a possible route to boost the transport properties and hence the specific power of lithium batteries [7]. We then address the conductivity of electrolytes directly relevant to the field of electrochemical storage systems: ILs charged with lithium salts. We show that these electrolytes confined in 1D CNT membranes show a drastic and unprecedented increase in ionic conductivity. Compared to the bulk analogues, we indeed report conductivity gains by a factor up to 50 upon macroscopic 1D CNT confinement.

Such a disruptive concept of a 1D CNT based separator laying at the cross-road of basic science is probably of interest for future technological outcomes.

- [1] Hayes, R., Warr, G. G. & Atkin, R. Structure and Nanostructure in Ionic Liquids. *Chem. Rev.* **115**, 6357–6426 (2015).
- [2] Lee, A. A., Vella, D., Perkin, S. & Goriely, A. Are Room-Temperature Ionic Liquids Dilute Electrolytes? *J. Phys. Chem. Lett.* **6**, 159–163 (2015).
- [3] Gebbie, M. A., Dobbs, H. A., Valtiner, M. & Israelachvili, J. N. Long-range electrostatic screening in ionic liquids. *Proc. Natl. Acad. Sci.* **112**, 7432–7437 (2015).
- [4] Ferdeghini, F. *et al.* Nanostructuration of ionic liquids: impact on the cation mobility. A multi-scale study. *Nanoscale* **9**, 1901–1908 (2017).
- [5] Quentin Berrod *et al.* Ionic Liquids: evidence of the viscosity scale-dependence. *Sci. Rep.* **7**, (2017).
- [6] Berrod, Q. *et al.* Enhanced ionic liquid mobility induced by confinement in 1D CNT membranes. *Nanoscale* **8**, 7845–7848 (2016).
- [7] Berrod, Q., Ferdeghini, F., Judeinstein, P. & Zanotti, J.-M. Nanocomposite membranes for electrochemical devices. Patent WO 2016151142 A1. (2016).

Augmented Reality in Neutron Experiments

M. Boehm¹, Y. Le Goc¹, T. Weber¹ and P. Mutti¹

¹ Institut Laue-Langevin, 71 avenue des Martyrs, 38042 Grenoble, France

Today's user community appreciates the active hand-on participation in experiments and the scientific exchange at the facilities, which act as international crossings for experts of very different scientific fields. Nevertheless, this way of access also imposes long missions on the users and puts time constraints on participants and instrument schedules, which hinders flexible handling of experiments or rapid integration of hot scientific topics. In future, a major severe constraint to the present user access arises from changing legislation, which has to assure increasing security standards for protecting nuclear installations and/or for protecting against misappropriation of materials on-site. Especially this last point might completely modify the future way of performing experiments and might have severe impact on the attractiveness of the technic as such.

Here, we suggest exploring state-of-the-art computing technology and develop an alternative, *virtual*, access mode for neutron experiments (NEVA). We suggest merging existing instrument control software, computing and scientific software tools, state-of the art communication technology and modern 3D animation into a new virtual platform. This platform would not concurrence existing tools for instrument control, data sorting and data analysis, but it will complement them. It will provide a generic interface for importing, illustrating and sharing information relevant to the experiments. In parallel to the virtual platform we envisage testing the usefulness of augmented reality at the instrument and experimental areas, for scientists and technical staff on-site. First concepts of a virtual platform have been successfully tested based on experience with existing single crystal inelastic neutron scattering software (TAKIN [1], vTAS [2]). NEVA will be open source and platform independent and usable with different instrumental techniques at the different facilities. The software will be a modern web application written in fast, just-in- time compiled Javascript.

[1] T. Weber, R. Georgii, P. Böni, SoftwareX 5 (2016), p. 121-126.

[2] M. Boehm, A. Filhol, Y. Raoul, J. Kulda, W. Schmidt, K. Schmalzl, E. Farhi, Nucl. Instr. and Meth. A 697 (2013), p. 40-44.

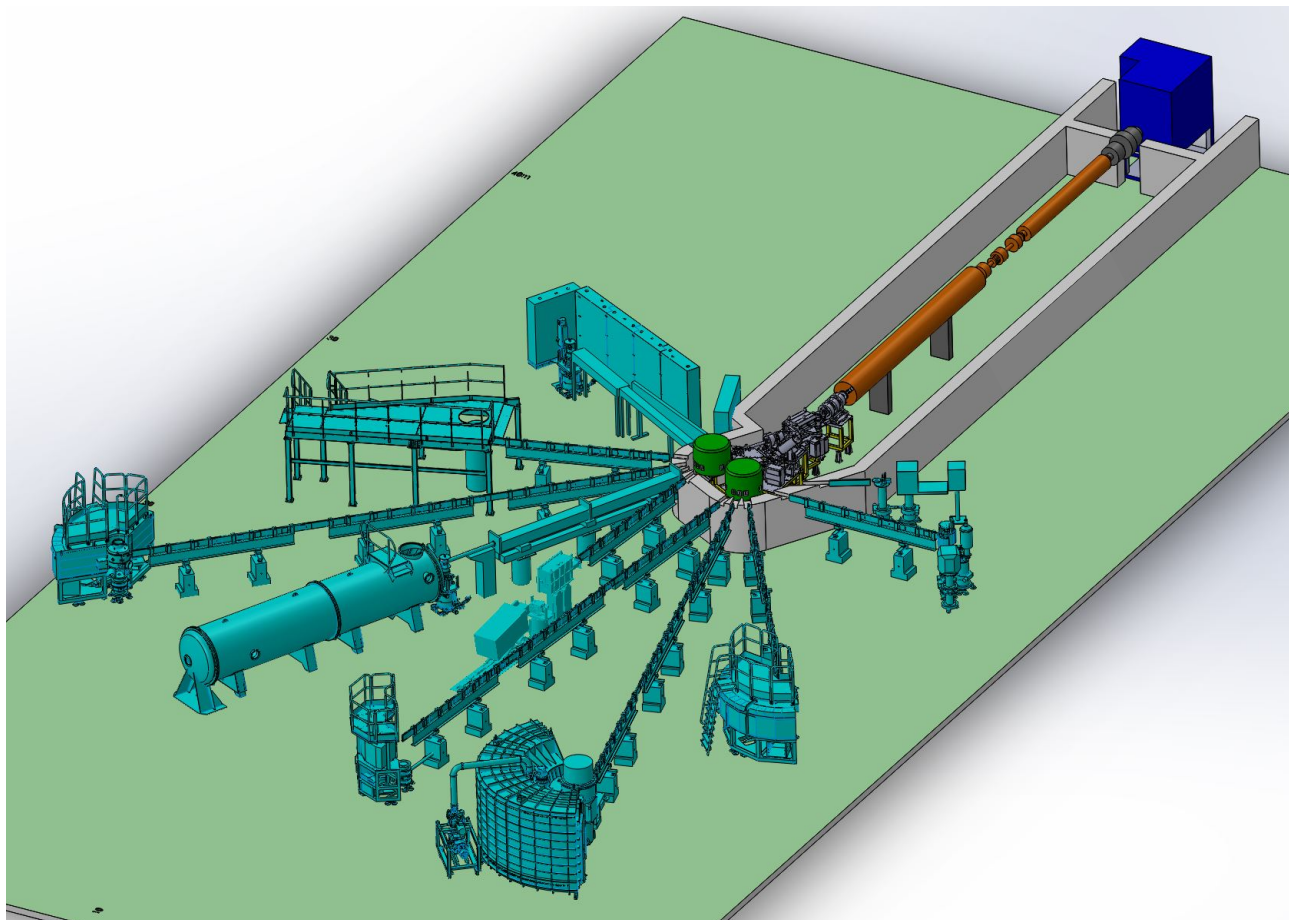
Quelle suite instrumentale sur une source compacte?

F. Ott

Laboratoire Léon Brillouin, CEA, CNRS, Université Paris-Saclay, 91191 Gif sur Yvette

Les développements technologiques permettent d'envisager la construction de sources de neutrons compactes dont le coût d'investissement est significativement plus faible que la construction d'un réacteur nucléaire ou d'une source à spallation. Diverses stratégies peuvent être envisagées, de la construction d'une source aux performances modestes en lien avec l'université avec une vocation de formation et une utilisation pour des expériences de caractérisation simples à une source à haute brillance dont les performances se comparent à une source à spallation ou un réacteur de puissance moyenne.

Les performances de différents types d'instruments seront présentées. Une discussion sur les différentes suites instrumentales envisageables en fonction de la puissance et des caractéristiques temporelles de la source sera ouverte.



CONDENSED MATTER

GEGGION

Physical-chemistry of gas hydrates : from astrophysics to new opportunities for energy technologies

A. Desmedt

Groupe Spectroscopie Moléculaire – Institut des Sciences Moléculaires UMR5255 CNRS – Univ. Bordeaux

Gas hydrates are ice-like systems made of a network of hydrogen-bonded water molecules (forming host cages) that is stabilized by the presence of foreign guest molecules [1]. The natural existence of large quantities of hydrocarbon hydrates in deep oceans and permafrost is certainly at the origin of numerous applications in areas such as energy and geophysics sciences and technologies [2]. Their hypothetical occurrence in extraterrestrial objects (planets, comets and planetesimal) is also the subject of numerous researches in astrophysics [3]. At a fundamental level, their nanostructuration confers on these materials specific properties (e.g. molecular selectivity, transport properties) for which the host-guest interactions play a key role [4,5]. These interactions occur on a broad timescale and thus require the use of multi-technique approach (Neutron scattering, Raman, NMR, Classical and *ab-initio* Molecular Dynamics Simulations). The presentation will review recent results obtained on the physical chemistry of clathrate hydrates towards two main issues - for which neutron scattering brings significant contributions: gas selectivity and structural metastability on one hand, and super-protonic conduction on the other hand.

Recent theoretical works suggest that the nitrogen depletion observed on the Jupiter family comet 67P/Churyumov-Gerasimenko might be due to preferential encapsulation of carbon monoxide with respect to nitrogen inside mixed gas hydrate [6]. The presentation will report the first experimental investigations of such a preferential trapping, together with unusual structural metastability, by means of Raman scattering and Neutron diffraction in various mixed gas (CO, CO₂, N₂) hydrates [7,8,9,10,11].

In addition to gaseous species, clathrate hydrates may encapsulate strong acids. Such supramolecular assembly leads to generate super-protonic conductors (i.e. with protonic conduction of the order of 0.1S/cm) [12]. Quasi-elastic neutron scattering is a unique technique for disentangling the proton transport mechanism involved in such ice-like systems [13,14]. This issue will be reviewed by outlining the contributions of Neutron scattering together with complementary techniques such as ab-initio Molecular Dynamics, Raman imaging or pulsed-field gradient proton NMR. Moreover, new opportunities in the area of energy (electrochemical energy production [15] and hydrogen storage [16,17,18]) are offered thanks to the strong acidic character of clathrate hydrates. These points will be outlined.

- [1] E. D. Sloan and C. A. Koh, Clathrate Hydrates of natural gases, Taylor & Francis-CRC Press, Boca Raton, FL, 3rd edn, 2008.
- [2] L. Ruffine, D. Broseta, A. Desmedt, Eds, Gas Hydrates 2: Geoscience Issues and Potential Industrial Applications, Wiley: London (2018).
- [3] e.g. G. Tobie *et al*, *Nature* 2006, 440, P.61 // *Nature* 2015, 519, p.162.
- [4] D. Broseta, L. Ruffine, A. Desmedt, Eds, Gas hydrates 1: Fundamentals, Characterization and Modeling, Wiley: London (2017).
- [5] A. Desmedt, *et al*. *Eur. Phys. J. Special Topics* 213 (2012) 103-127
- [6] S. Lectez, *et al*, *Astrophys. J. Lett.*, 2015, 805: L1.
- [7] C. Petuya, *et al*, *J. Phys. Chem. C* 121(25) (2017) 13798–13802
- [8] C. Petuya, *et al*, *J. Phys. Chem. C* 122(1) (2018) 566 –573
- [9] C. Petuya, *et al*, *Crystals* 8 (2018) 145(1-13)
- [10] C. Petuya, *et al*, *Chem. Comm.* 54 (2018) 4290-4293.
- [11] C. Petuya, *et al*. Submitted to PCCP (2018).
- [12] J. Cha, *et al*. *J. Phys. Chem. C* 2008, 112, 13332–13335.
- [13] L. Bedouret, *et al*, *J. Phys. Chem. B* 118 (2014) 13357–13364.
- [14] A. Desmedt, *et al*, *Solid State Ionics*, 252 (2013) 19-25
- [15] S. Desplanche *et al*, in preparation.
- [16] E. Pefoute, *et al*, *J. Phys. Chem. C* 116(32) (2012) 16823
- [17] A. Desmedt, *et al*, *J. Phys. Chem. C* 119 (2015) 8904-8911
- [18] T.T. Nguyen, *et al*, in preparation.

Anomalous crystal field splitting in antiferro-quadrupolar compound TmTe and isostructural $Tm_{0.1}Yb_{0.9}Te$

E. Clementyev^{1,2} and J.-M. Mignot³

¹ I. Kant Baltic Federal University, Kaliningrad, Russia

² Petersburg Nuclear Physics Institute, Gatchina, St-Petersburg, Russia

³ Laboratoire Léon Brillouin, CEA-CNRS, CEA/Saclay, France

The Tm monochalcogenide family displays exotic physical properties including valence instabilities and quadrupolar ordering. In particular TmTe was reported to undergo a phase transition at $T_Q=1.7K$ above the magnetic ordering temperature ($T_N=0.4K$). One of the most crucial questions is the origin of the ground state of the Tm^{2+} 4f multiplet in TmTe (see [1] and references therein). A lack of experimental consensus regarding the the detailed level sequence of the crystal field level scheme is a significant problem. Experimental data collected on pure TmTe show relatively broad crystal field transitions below 1 meV (INS measurements have been performed on the 4F1 triple-axis spectrometer (LLB, Saclay). To avoid the broadening due to the quadrupolar correlations the measurements on a diluted compound, namely 10% Tm impurity in the nonmagnetic YbTe matrix have been performed on the time-of-flight spectrometer FOCUS (SINQ, PSI). The incoming neutron energy was 3.27 meV yielding the energy resolution at the elastic position of about 0.1 meV. For the first time two distinct crystal field transitions have been observed (at $E\sim 0.3$ meV and $E\sim 0.9$ meV) in TmTe-based system. Such a spectrum is unique since the total magnitude of the crystal field splitting is one or even two orders of magnitude smaller than in the majority of the 4f systems and in isostructural metallic $Tm_xLa_{1-x}Te$ systems [2]. The observed effects are opposite to the predictions of the point charge and related models. The puzzling small magnitude of the total crystal field splitting in TmTe is discussed.

[1] R. Shiina and N. Tatsuya, J. Phys. Soc. Jpn., vol: 77, num: 12 (2008) 124715/1-124715/6.

[2] T. Matsumura et al., Phys. Rev. B 66 (2002) 104410.

Combined Solid-State NMR and Neutron Diffraction Study Strontium-Aluminosilicate glasses: towards NMR driven RMC

Thibault Charpentier,¹ Louis Hennet,² Kirill Okhotnikov,¹ Pierre Florian,² Frank Fayon,² Alexey Novikov,² Jacques Darpentigny,³ Maxime Van loon,² Daniel Neuville.⁴

¹ NIMBE, CEA, CNRS, Université Paris-Saclay, CEA Saclay, France.

² CNRS, CEMHTI UPR3079, Univ. Orléans, France.

³ Laboratoire Léon Brillouin, CEA-CNRS, CEA Saclay, France.

⁴ CNRS-IPGP, Paris Sorbonne Cité, France.

The structure of aluminosilicate $\text{SiO}_2\text{-Al}_2\text{O}_3\text{-SrO}$ based glass compositions which are largely unexplored systems[1,2] has been investigated using solid-state NMR combined with neutron diffraction measurements. Glasses on the compensation line $[\text{Al}_2\text{O}_3]=[\text{SrO}]$, were studied with ^{17}O , ^{29}Si and ^{27}Al solid state NMR at high (11.7 T) and very-high (20.0 T) magnetic fields, together with neutron diffraction data collected on the 7C2 diffractometer[3] at the LLB (Laboratoire Léon Brillouin).

Classical and ab-initio molecular dynamics (MD) simulations were performed. In agreement with experimental data, MD simulations predict that aluminium is predominantly tetrahedrally coordinated for all the studied compositions with a small fraction of AlO_5 units ranging from 2 to 5%.

Using the MD models, DFT calculations of NMR parameters were performed. Computed NMR parameters were linked to local structural features to establish relationships between experimental NMR spectra and the underlying topological disorder. For example, quantitative relationships between bond-angles, bond-distances, Al/Si mixing and NMR fingerprints of ^{29}Si and ^{27}Al could be established. In parallel, the Al/Si connectivities were investigated using advanced NMR techniques enabling the resolution of the ^{29}Si NMR spectrum in terms of Qn(mAl) units (i.e., Qn connected to m Al units).

In order to integrate the NMR information in the modelling process together with the neutron data, not only the coordination numbers but also constraints from Al/Si mixing, NMR-derived bond-angle distributions, we have devised a new code aiming at performing a NMR driven Reverse Monte Carlo procedure that we are currently developing and includes standard MD potentials. Results will be presented highlighting the crucial contribution of NMR information.

[1] A.N. Novikov, D.R. Neuville, L. Hennet, Y. Gueguen, D. Thiaudière, T. Charpentier, P. Florian, Al and Sr environment in tectosilicate glasses and melts: Viscosity, Raman and NMR investigation, *Chem. Geol.* 461 (2017) 115–127. doi:10.1016/j.chemgeo.2016.11.023.

[2] L. Cormier, G. Calas, S. Creux, P.H. Gaskell, B. Bouchet-Fabre, A.C. Hannon, Environment around strontium in silicate and aluminosilicate glasses, *Phys. Rev. B* 59 (1999) 13517–13520. doi:10.1103/PhysRevB.59.13517.

[3] G.J. Cuello, J. Darpentigny, L. Hennet, L. Cormier, J. Dupont, B. Homatter, B. Beuneu, 7C2, the new neutron diffractometer for liquids and disordered materials at LLB, *J. Phys. Conf. Ser.* 746 (2016) 012020. doi:10.1088/1742-6596/746/1/012020.

Elastic softness of hybrid lead halide perovskites

A.C. Ferreira^{1,2}, A. Létoublon², S. Paofai³, S. Raymond⁴, C. Ecolivet⁵, B. Rufflé⁶, S. Cordier³, C. Katan³, M. I. Saidaminov⁷, A. A. Zhumekenov⁷, O. M. Bakr⁷, J. Even² and P. Bourges¹

¹ Laboratoire Léon Brillouin, CEA-CNRS, Université Paris-Saclay, CEA Saclay, 91191 Gif-sur-Yvette, France

² Laboratoire FOTON, INSA, Université Rennes, F35708 Rennes, France

³ Institut des Sciences Chimiques de Rennes, CNRS, Université de Rennes 1, Ecole Nationale Supérieure de Chimie de Rennes, INSA de Rennes, 35042 Rennes, France

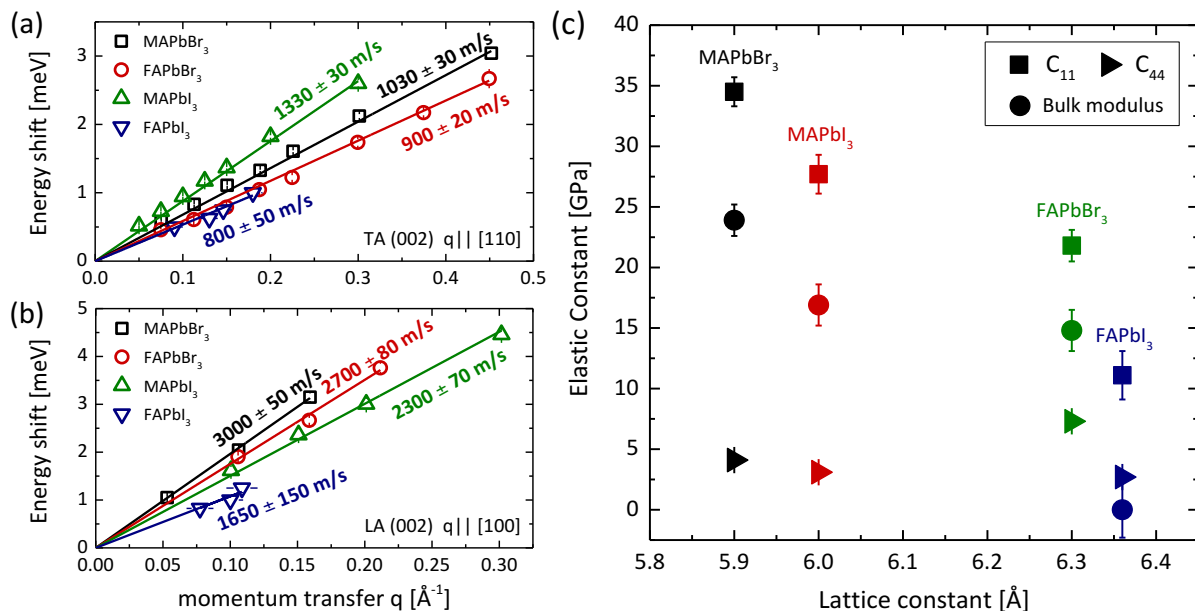
⁴ Univ. Grenoble Alpes, CEA, INAC, MEM, 38000 Grenoble, France

⁵ Institut de Physique de Rennes, CNRS, Université de Rennes 1, 35042 Rennes, France

⁶ Laboratoire Charles Coulomb, UMR 5221, Université de Montpellier, 34095 Montpellier, France

⁷ King Abdullah University of Science and Technology (KAUST), KAUST Catalysis Center, KAUST Solar Center, Physical Sciences and Engineering Division (PSE), Thuwal 23955-6900, Saudi Arabia

Hybrid organic-inorganic perovskites (HOP) have been intensively studied as promising materials for photovoltaic applications, taking advantage of their high efficiency and low cost processing. Although much recent attention has also been devoted towards unraveling their microscopic optoelectronic properties, the origin of their softness, by comparison to classic semiconductors, is currently still lacking a comprehensive understanding and systematic experimental studies. Here we investigate by coherent inelastic neutron scattering spectroscopy and Brillouin light scattering, low frequency acoustic phonons in four different hybrid perovskite single crystals: MAPbBr₃, FAPbBr₃, MAPbI₃ and α -FAPbI₃. We report a very small shear C_{44} elastic constant for all the compounds and a considerable elastic anisotropy. The extremely low bulk modulus and negative C_{12} in α -FAPbI₃ substantiates its very unstable nature and in FAPbBr₃, a tendency towards an incipient ferroelastic transition, is interpreted as further evidence of the influence of plasticity in hybrid perovskites. We observe a systematic lower sound group velocity in the technologically important iodide-based compounds compared to the bromide-based ones. The findings suggest that low thermal conductivity and hot phonon bottleneck phenomena are expected to be enhanced by low elastic stiffness, particularly in the case of the ultrasoft α -FAPbI₃. This project has received funding from the European Union's Horizon 2020 programme, through a FET Open research and innovation action under the grant agreement No 687008.



Acoustic phonon dispersion curves of the four HOP (a) transverse acoustic (TA) and (b) longitudinal acoustic (LA) phonons close to the (002) Bragg reflection, measured by INS. (c) Elastic constants C_{11} and C_{44} (black) as well as the bulk modulus K (red) behaviour as a function of the changing lattice constant between compounds.

Phase diagram and redox behavior of $(\text{Nd}/\text{Pr})_2\text{NiO}_{4+\delta}$ electrodes explored by *in situ* neutron powder diffraction during electrochemical oxygen intercalation

M. Ceretti¹, O. Wahyudi^{1,2}, G. André³, M. Meven⁴, A. Villesuzanne², W. Paulus¹

¹ Institut Charles Gerhardt Montpellier, UMR 5253 CNRS-UM-ENSCM, Université de Montpellier, Place Eugène Bataillon, 34095 Montpellier Cedex 5, France.

² CNRS, Université de Bordeaux, ICMCB, UMR5026, 87 Av. Dr. A. Schweitzer, 33608 Pessac Cedex, France

³ Laboratoire Léon Brillouin, UMR12, CEA-CNRS, CEA Saclay, 91191 Gif Sur Yvette, France

⁴ Institute of Crystallography, RWTH Aachen University and Jülich Centre for Neutron Science (JCNS) at Heinz Maier-Leibnitz Zentrum (MLZ), 85747 Garching, Germany

Oxygen intercalation/deintercalation in $\text{Pr}_2\text{NiO}_{4+\delta}$ and $\text{Nd}_2\text{NiO}_{4+\delta}$ was followed by *in situ* neutron powder diffraction during electrochemical oxidation/reduction, in a dedicated reaction cell at room temperature [1]. For both systems three phases, all showing the same line-width, were identified.

The starting phases, $\text{Pr}_2\text{NiO}_{4.23}$ and $\text{Nd}_2\text{NiO}_{4.24}$, considered with an average orthorhombic $Fmmm$ symmetry, although both show a slight monoclinic distortion, get reduced in a 2-phase reaction step to tetragonal intermediate phases with $0.07 \leq \delta \leq 0.10$ and $P4_2/ncm$ space group, which on further reduction transform, again in a 2-phase reaction step, towards the respective stoichiometric $(\text{Pr}/\text{Nd})_2\text{NiO}_{4.0}$ phases, with $Bmab$ space group. Electrochemical oxidation does, however, not proceed fully reversibly for both cases: while the re-oxidation of $\text{Nd}_2\text{NiO}_{4+\delta}$ is limited to the tetragonal intermediate phase with $\delta = 0.10$, the homologous $\text{Pr}_2\text{NiO}_{4+\delta}$ can be re-oxidized up to $\delta = 0.17$, showing orthorhombic symmetry. For the intermediate tetragonal phase, we were able to establish for $\text{Pr}_2\text{NiO}_{4.09}$ complex anharmonic displacement behaviour of the apical oxygen atoms, as analysed by single crystal neutron diffraction and Maximum Entropy Analysis, in agreement with a low-T diffusion pathway for oxygen ions, activated by lattice [2-3].

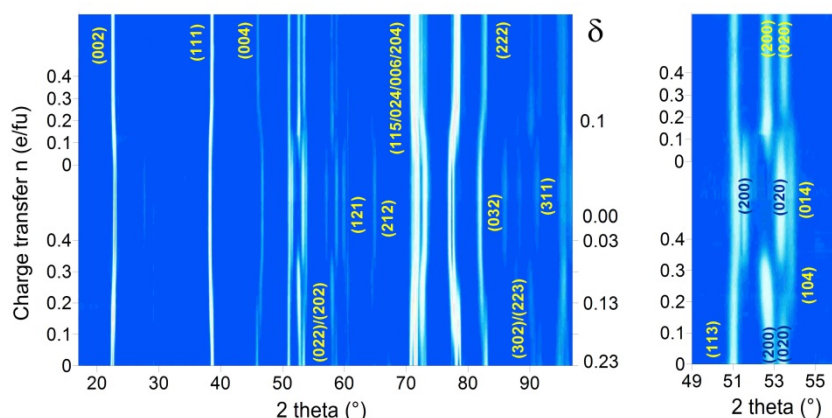


Figure 1. Neutron powder diffraction patterns obtained *in situ* during the electrochemical reduction-oxidation of $\text{Pr}_2\text{NiO}_{4+\delta}$ (G41, $\lambda = 2.422(2)\text{\AA}$). In the right part, zoom-in view of the diffraction patterns

[1] M. Ceretti, O. Wahyudi, G. André, M. Meven, A. Villesuzanne, W. Paulus, Inor. Chem., (2018), DOI: 10.1021/acs.inorgchem.8b00393

[2] M. Ceretti, O. Wahyudi, A. Cousson, A. Villesuzanne, M. Meven, B. Pedersen, J. M. Bassat, W. Paulus, J. Mat. Chem. A, (2015), 21140-21148

[3] A. Piovano, A. Perrichon, M. Boehm, M. R. Johnson, W. Paulus, Phys. Chem. Chem. Phys., (2016), 17398-17403

POGTER

GEGGION

Conformation of grafted polymer chains in nanoporous membrane

Erigene Bakangura^a, Nicolas Jouault^b, Anastasia Christoulaki^b, Alexis Chennevière^a

^a Laboratoire Léon Brillouin (CEA-CNRS), CEA Saclay, 91191 Gif-sur-Yvette Cedex,

^b Laboratoire PHENIX, Sorbonne Université, 4 place Jussieu — 75252 Paris Cedex 5, FRANCE

Nanoporous anodized aluminum oxide membrane (AAO) is one of the most popular nanomaterial because of its simple, cheap and well controlled fabrication process. For example, several studies showed that grafting or adsorbing polymer chains within the pores can influence significantly the flow of simple liquids, translocation rate of polymer chains or even ionic conductivity[1]. On the fundamental point of view, several studies managed to characterize the brush extension on flat and convex surfaces[2]–[4]. These studies highlighted a very good agreement between the experimental studies and the scaling law model developed by Alexander, De Gennes, Daoud and Cotton. However, regarding concave polymer brush, there is still a theoretical debate on the validity of the Daoud-Cotton model for such systems [5]. Here, we used small angle neutron scattering in order to probe the conformation of end-grafted polystyrene chains within AAO nanopores with diameter ranging from 20 to 60 nm. We show that the molecular weight of grafted chains and their grafting density influence the form factor of the pores.

As a complementary characterization, we determined the hydrodynamic radius of the grafted nanopores by measuring the flow rate at constant pressure drop. The comparison of both SANS and flow permeability experiment allows to couple molecular insight and transport properties of grafted nanoporous membrane.

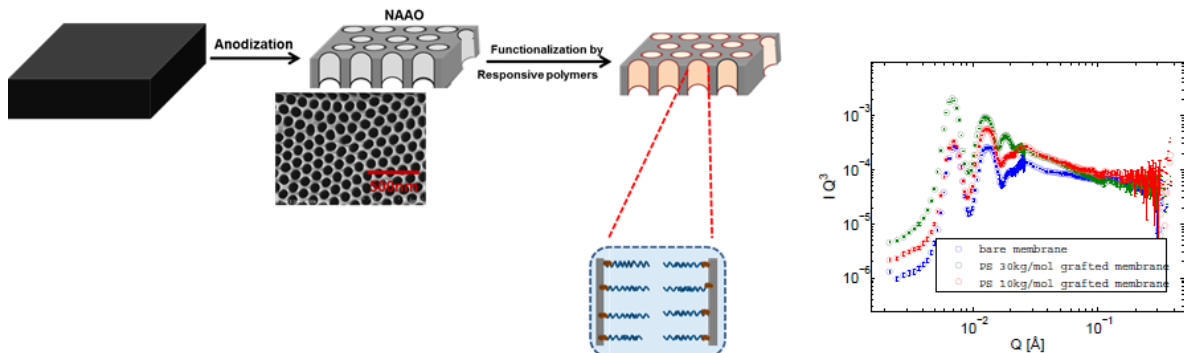


Figure 1 :(left) : Synthesis scheme of polymer grafted aluminum oxide nanoporous membrane
(right) : SANS spectra of bare membrane and grafted PS-NH₂ which molecular weights are 10kg/mol and 30 kg/mol immersed in a mixture of THF-h and THF-d (31.1 %/ 69.9 %

- [1]. Md Jani, et al. . Prog. Mater. Sci. 58, 636–704 (2013).
- [2]. Lal, J., et al., J. Phys. II 7, 19 (1997).
- [3]. Auroy, P. et al., . J. Phys. II 3, 227–243 (1993).
- [4]. Marzolin, C. et al. . Macromolecules 34, 8694–8700 (2001).
- [5]. Manghi, M., et al., Eur. Phys. J. E 5, 519–530 (2001).

Drying of nanocomposites : interplay between structure and rheological behaviour

ERMAN A.^{1,2}, LE COEUR C.^{1,3}; AMIEL C.¹; LORTHIOIR C.^{1,4}; FALL A.²; OVARLEZ G.⁵

¹*ICMPE, Thiais*

²*Laboratoire Navier, Champ sur Marne*

³*Laboratoire Léon Brillouin, CEA Saclay, Gif-sur-Yvette*

⁴*Laboratory Of Future, Pessac*

The dispersion of nanoscale inorganic fillers in a polymer matrix may potentially lead to a significant improvement of certain mechanical properties of the material. One of the ways to prepare these nanocomposite materials is based on solvent evaporation. The formation of the microstructure during the drying process remains a poorly understood phenomenon. To address this question, we chose a system based on a water-soluble polymer, poly(methacrylic acid), the conformation of which is pH dependent, and silica nanoparticles with well-controlled size, well-known geometry and various surface functionalization, in aqueous solvent.

The purpose is to monitor the drying of these materials and to study their evolution toward the solid state. The results obtained should help to understand the mechanisms involved during drying, their impact on the filler dispersion and the mechanical behavior of the final nanocomposites.

First, mixtures of polymer-silica in solution were made. Variables are pH and concentrations with a mass ratio polymer/silica fixed at 4/1. Three phase diagrams were obtained for three different silica nanoparticles with different surface groups so that interactions between polymer and silica may be tuned. Every solutions were then characterized by Small Angle X-ray Scattering and by Small Angle Neutron Scattering. These two experiments allowed us to get information about silica structure or polymer conformation within the mixtures. The presence of aggregates can be confirmed by analyzing the form factor and the structure factor.

Physical hybrid hydrogels with Pickering emulsion as cross-linker: a new smart system

F. Ferdeghini^{1,2}, Z. Guennouini^{1,2}, C. Le Cœur^{2,3} and F. Muller^{1,2}

¹ LICORNE, ECE-Paris, 37 boulevard de Grenelle 75015 Paris

² Laboratoire Léon Brillouin (CEA-CNRS), CEA Saclay, 91191 Gif-sur-Yvette cedex

³ ICMPE, 2 rue Henry Dunant 94320 Thiais

Due to their high-water content, hydrogels are very promising for the biocompatible applications. However, these systems show very poor mechanical properties because of the large amount of water. This limitation has been overpassed by synthetizing the polymer chains in presence of inorganic nanoparticles (NPs). These latter act as physical cross-linkers and enhance remarkably the mechanical properties^[1].

We recently extended the formulation of such a system by using lipid liquid crystalline (LC) phases stabilized by hectorite nanoplatelets^[2,3]. As many polymers can be adsorbed on the platelets' surfaces, we could exploit this affinity to form a tridimensional polymeric network using the emulsion's drops as cross-linkers (Fig.1). These systems are very interesting for drug delivery-based applications since molecules both hydrophobic and hydrophilic can load the LC phases.

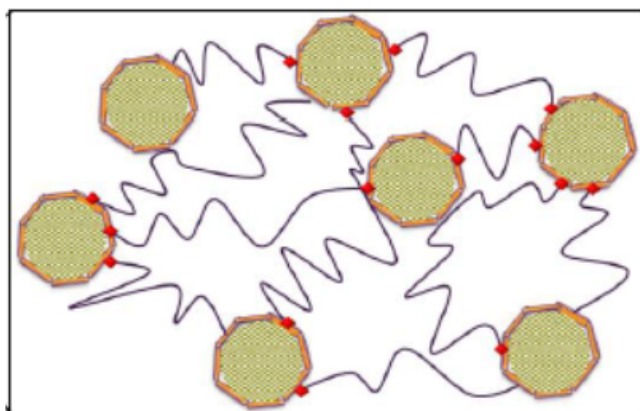


Figure 2 Schematic representation of the hydrogels cross-linked by the LC emulsion. The emulsion's drops are composed by the lipid LC phase (checked circles), which is surrounded by the nanoplatelets (brown cylinders). The polymers chains (dark lines) can be adsorbed on the NPs surface forming a 3D network.

The goal of this work is the investigation of the correlation between the mechanical and structural properties of Polyacrylamide-based hydrogels cross-linked by the LC stabilized emulsion.

We performed dynamic mechanical analysis (DMA) and rheology measurements in order to determine the effect of the crosslinking on the mechanical properties of these systems at the macroscopic scale. We observed a remarkable enhancement of the Young and Shear moduli due to the interaction between the polymer chains and the emulsion's drops.

We completed our study by performing neutrons and X-rays small angles scattering measurements in order to observe the effects of the mechanical deformation on the hydrogels' structural organization at the nm scale. We observed that the mechanical stress has a remarkable impact to emulsion's structure. First in the low-medium deformation range, the emulsion's drops shape seems to become anisotropic evolving from sphere to an ellipsoid in the direction of the stress. Furthermore for elevate deformation (at the elongation rate higher than 100%) the mechanical stress seems to induce an anisotropy at the lipid LC phase.

[1] Haraguchi, K. *et al.*, *Macromolecules*, 35 (2002), 10162–10171.

[2] Salonen A. *et al.*, *Langmuir*, 24 (2008), 5306-5316.

[3] Muller F. *et al.*, *Soft Matter*, 8 (2012) 10502-10510.

Implementation of nanoporous alumina membranes for the confinement of polyelectrolytes

A. Christoulaki ¹, A. Chennevière ² E. Dubois ¹ and N. Jouault ¹

¹ Sorbonne Université, Laboratoire PHENIX, F-75005, Paris, France

² Laboratoire Léon Brillouin (LLB), CEA Saclay, 91191 Gif-Sur-Yvette, France

Nanoporous materials can be used as media for studying confinement of soft matter. Among them, nanoporous alumina membranes (nPAM) are promising model systems for such studies. The nPAMs are synthesized by electrochemical anodization of aluminum and consist of parallel nanochannels with monodisperse diameters that are arranged in a hexagonal lattice and whose size is directly tunable by the synthesis conditions. Moreover, nPAM is an amphoteric material whose charge behavior depends on the pH, thus providing both geometrical and electrostatic confinement.

The conformation and dynamics of soft matter can be addressed by Small Angle Neutron Scattering (SANS). However, before studying the behavior of guest species inside a host medium, it is essential to characterize the confining medium. For this reason, the nPAM were characterized by SANS by utilizing the well-known method of contrast variation from which information on the structure and chemical composition can be extracted. The characterization of such highly dense ordered structures is non-trivial and a detailed strategy will be proposed in order to avoid multiple scattering effects and “match” the nPAM since there is no contrast matching point where the nPAM scattering intensity “eliminates”. Our results show that the nPAM contains two layers with different composition and are radially distributed around the pore axis, forming a contamination shell. Fitting of the SANS experimental data provides the basic geometrical characteristics such as the pore diameter, interpore distance and the extent of the contamination shell. The fitting model that includes a hexagonal structure factor with a form factor of a core-shell cylinder will be detailed (see Fig. 1).

Finally, we will present some SANS data to study the behavior of sodium polystyrene sulfonate (NaPSS) inside nPAM having different pore sizes and charges.

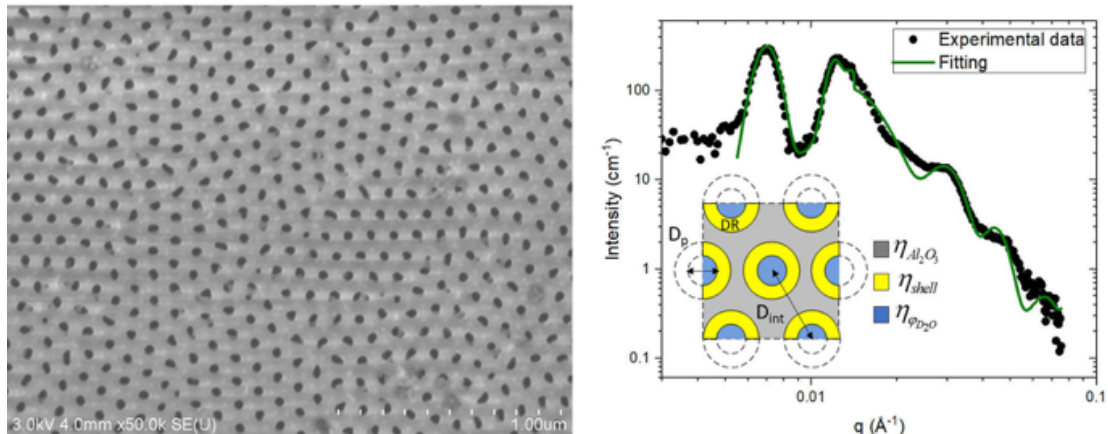


Figure 1: Left: SEM image of a nPAM. Right: SANS data of a nPAM and the corresponding fitting with a core-shell cylinder model.

Powder neutron diffraction study of $\text{YbMn}_{6-y}\text{Fe}_y\text{Sn}_6$ alloys ($y \leq 1.25$)

A. Magnette¹, T. Mazet¹, L. Eichenberger¹, A. Vernière¹, B. Malaman¹, G. Venturini¹, and V. Nassif²

¹ Institut Jean Lamour, CNRS (UMR 7198) – Université de Lorraine, 54011 Nancy Cedex, France.

² Institut Laue Langevin, CS 20156, 38042 Grenoble Cedex 9, France

The ferromagnetic YbMn_6Sn_6 compound ($T_c \sim 290$ K) contains a non-magnetic intermediate valent Yb ($v \sim 2.6$) [1]. It crystallizes in the SmMn_6Sn_6 type of structure ($P6/mmm$), a partially disordered variant of HfFe_6Ge_6 ($P6/mmm$).

We have investigated the new $\text{YbMn}_{6-y}\text{Fe}_y\text{Sn}_6$ alloys ($y = 0.25, 0.50, 0.75, 1.00$ and 1.25). The Fe doping alters both the crystal and magnetic properties. All alloys crystallize in the orthorhombic ($Imm\bar{m}$) HoFe_6Sn_6 type of structure [2], a long range ordered superstructure of HfFe_6Ge_6 . Yb keeps its non-magnetic intermediate valent character. Because of the Valence Electron Concentration increases, the Fe doping yields the development of a low-temperature antiferromagnetic-like state, whose temperature extent growths with the Fe content to cover the whole magnetically ordered temperature range for high enough Fe contents.

The data collected with the D1B diffractometer (ILL, Grenoble, France) indicate that these phases adopt helimagnetic arrangements with $\mathbf{k} = (0, q_y \sim 0.25, 0)$. This is the first time that incommensurate magnetic arrangements are observed in non- HfFe_6Ge_6 -type 1:6:6 compounds.

[1] L. Eichenberger *et al.*, J. Alloys Compd., 695 (2017) 286

[2] A. Magnette *et al.*, J. Magn. Magn. Mater., 458 (2018) 19

Structural resolution of inorganic nanotubes and water confinement in hydrophilic/hydrophobic nanochannels

G.Monet¹, M.S.Amara¹, E.Paineau¹, S.Rouzière¹, Z.Chai², G.Teobaldi³, S.Rols⁴ and P.Launois¹

¹ Laboratoire de Physique des Solides, UMR CNRS 8502, Université Paris Sud, Université Paris Saclay, 91405 Orsay Cedex, France

² Beijing Computational Science Research Centre, 100193 Beijing, China

³ Stephenson Institute for Renewable Energy and Department of Chemistry, The University of Liverpool, L69 3BX Liverpool, United Kingdom

⁴ Institut Laue-Langevin, BP 156, 38042 Grenoble, France

A groundbreaking discovery in nanofluidics was the observation of the tremendously enhanced water permeability of carbon nanotubes, at the origin of an intensive research activity. But experimental studies about the role of the nanocontainer curvature and of liquid-surface interactions on the unique properties of nano-confined water are still scarce.

Within this context, we considered metal-oxide imogolite nanotubes of nominal composition $(\text{OH})_3\text{Al}_2\text{O}_3\text{Si}(\text{Ge})\text{OH}$ as a new host of confined water. Indeed, unlike carbon nanotubes, the electrostatic interaction can be tuned by functionalizing hydrophilic wall by hydrophobic methyl groups [1]. Thanks to their chemical versatility, imogolite nanotubes are promising candidates to understand the liquid-surface interactions and for applications in molecular storage, recognition and separation [2].

Yet, the determination of the atomic structure of inorganic single-walled nanotubes with complex stoichiometry remains elusive due to the too many atomic coordinates to be fitted with respect to X-ray diffractograms inherently exhibiting rather broad features. Thus, we introduce a new approach which enables resolution of their structure [3]. It is based, first, on the use of helical symmetries allowing one to consider the smallest unit cell and then on semi-empirical energy minimization leading to a reduction of the number of structural parameters to be fitted. Fit of wide-angle X-ray scattering (WAXS) diagrams of recently synthesized methylated alumino-silicate and alumino-germanate $(\text{OH})_3\text{Al}_2\text{O}_3\text{Si}(\text{Ge})\text{CH}_3$ enabled us to determine their atomic structure. We show that unlike their (N,0) zigzag hydroxylated analogs $(\text{OH})_3\text{Al}_2\text{O}_3\text{Si}(\text{Ge})\text{OH}$, methylated imogolite nanotubes roll up into a (N,N) armchair structure. Finally, combining X-ray scattering, thermogravimetric analyses and inelastic neutron scattering up to 273K alongside DFT simulations, we revealed multi-step process dehydration phenomenon and water structuration in layers in metal-oxide imogolite nanotubes [4]. The peculiar hydrogen bonding network, its specific vibrational properties and ‘phase transitions’ of confined water will be also discussed.

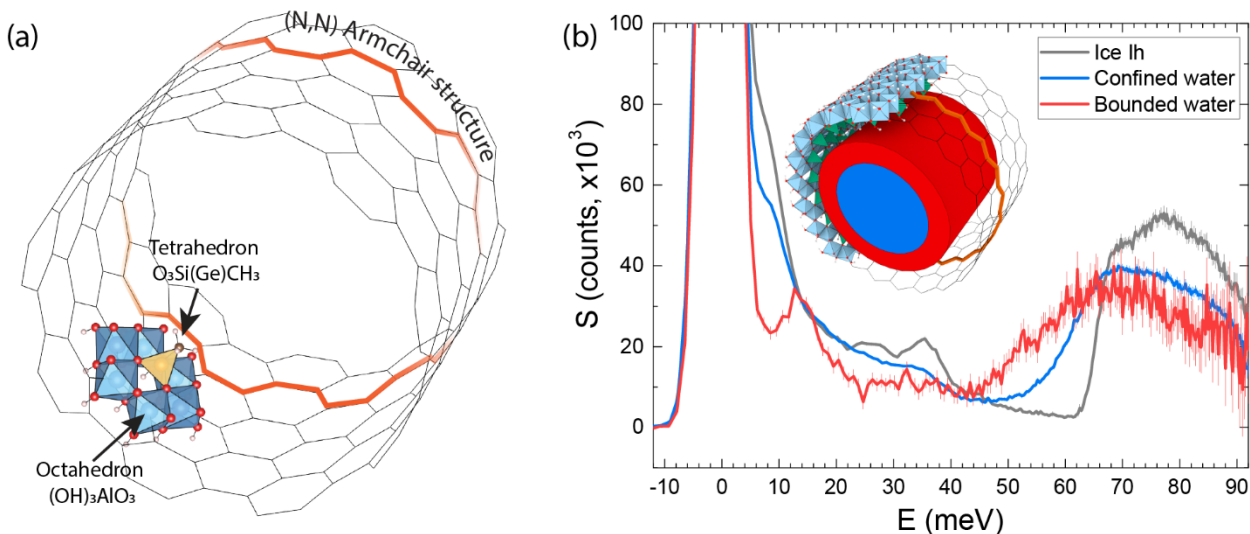


Figure: (a) The methylated imogolite nanotube structure. Its armchair character is highlighted by the thick orange line. (b) Dynamical structure factors $S(E)$ of confined (in blue) and bond water (in red) in hydroxylated alumino-germanate imogolite nanotube. They are compared to that measured for bulk ice Ih (in grey). The structure of the related (N,0) zigzag imogolite nanotube and the water structuration in layers is also depicted.

[1] M.S.Amara et al, Chem of Mat, 27 (2015) 1488-1494

[2] D.-Y.Kang et al, Nat Commun, 5 (2014) 3342

[3] G.Monet et al, to be published in Nat Commun, (2018)

[4] Article in preparation

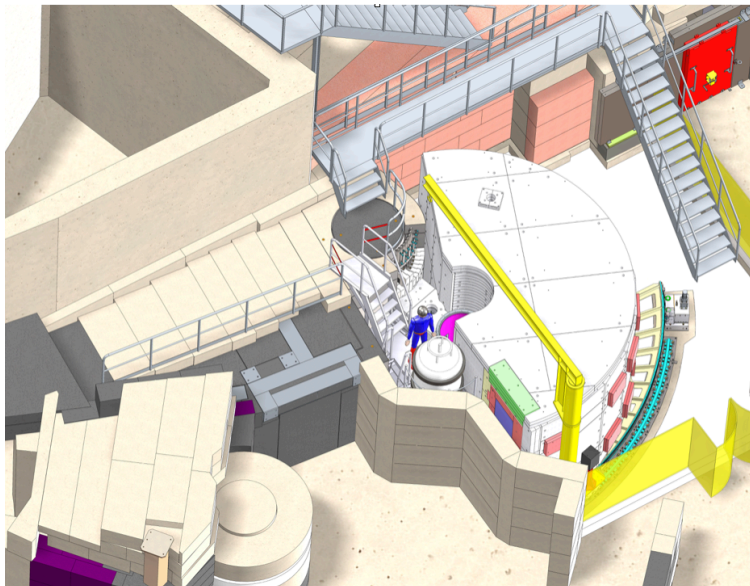
PANTHER: a thermal time of flight spectrometer at the ILL

G. Manzin, B. Fåk, B. Jarry, O. Meulien, ... S. Rols... et al.

Institut Laue-Langevin, BP 156, 38042 Grenoble, France

PANTHER (Polarization ANalysis on a THERmal time-of-flight) is a multi-purpose direct geometry thermal neutron time-of-flight (TOF) spectrometer optimized for studies of magnetism, single crystals, and small samples. Its high neutron flux, medium resolution, large detector coverage, and wide span of incoming energies allows for fast mapping of magnetic and structural excitations over a large range of wave-vector and energy transfers. PANTHER will allow for the use of complex sample environment, including the 10 Tesla « IN5 » magnet. It will also be equipped with full longitudinal polarization analysis using a ^3He -filter device (PASTIS-3). The instrument will be built at the H12 beam tube and will replace IN4C.

Compared to IN4C, the main improvements are the use of position-sensitive detectors (PSD), a well-shielded flight chamber connected to a wide-diameter sample area with a common vacuum, fully double focusing monochromators, additional background choppers, and non-magnetic construction materials. This will lead to a gain in flux of about two, an increased solid area of a factor of three, and a reduced background by a factor of ten. The improved signal-to-noise ratio of 60 will be profitable for studies of magnetism, lattice dynamics, and vibrational spectroscopy in the incoming energy range 6-120 meV. The use of ^3He PSD's will allow for single-crystal studies.



Unexpected magnetic field behaviour of spin stripes in LSCO superconductor close to the underdoped quantum critical point

Ana Elena Tătăreanu^{1,2}, Martin Böhm¹, Paul Steffens¹, Tim Tejsner^{1,2}, Monica Lăcătușu^{2,3}, Jean Claude Grivel³, Laura Folkers⁴, Yasmine Sassa⁵, Kim Lefmann²

¹Spectroscopy, Institut Laue Langevin, Grenoble, FR.

²Niels Bohr Institute, University of Copenhagen, Copenhagen, DK.

³Department of Energy Conversion and Storage, Technical University of Denmark, Kongens Lyngby, DK.

⁴Centre for Analysis and Synthesis, Lund University, Lund, SE.

⁵Department of Physics and Astronomy, Uppsala University, Uppsala, SE.

For the past 30 years, considerable scientific effort has been put into the quest of understanding the mechanism behind high temperature superconductivity. It is believed that clues to the pairing mechanism, can be found in understanding the interplay between spin and charge orders and superconductivity in ceramic cuprates superconductors [1]. Our group is currently investigating the behaviour of spin density waves, so called spin stripes, in highly underdoped $\text{La}_{2-x}\text{Sr}_x\text{CuO}_4$ (LSCO) superconducting single crystals ($0.05 < x < 0.09$). In our most recent neutron scattering experiments we have not observed static stripes signal in a $x=0.08$ LSCO single crystal, disputing the general belief that magnetic order is present for all dopings below $x=0.135$ [2]. This could be an indication that, in the extremely underdoped region of the LSCO phase diagram, it is not the same ordering phenomena that generates the static and dynamic magnetic stripes. Contrary to all evidence from literature, where a magnetic field is reported to produce an enhancement of low-energy fluctuations in LSCO samples with $x=0.105$ [4], $x=0.163$ [5] and $x=0.18$ [6] or no effect for $x=0.12$ [7] (Fig. 1), our $x=0.08$ LSCO single crystal showed a low energy (<1.5 meV) suppression of the dynamic magnetic stripes signal by an applied magnetic field (Fig 1). Going further, we plan to make a detailed study of the magnetic stripes on both sides of the QCP.

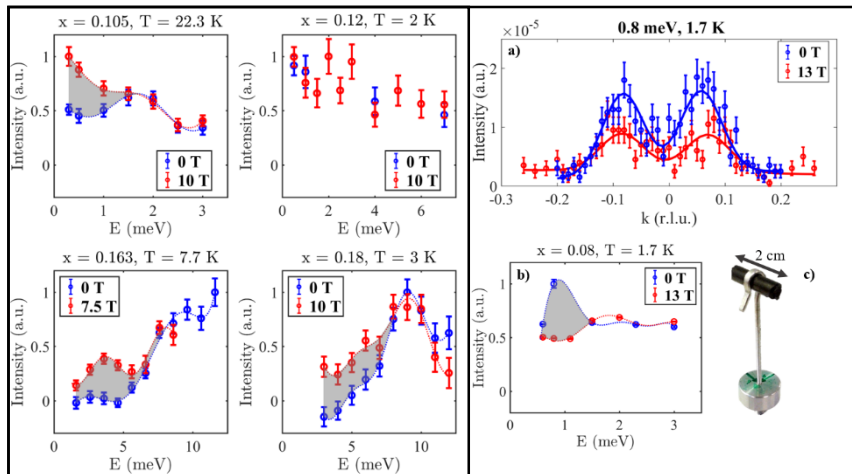


Figure 1: (left panel) Applied magnetic field dependence of the spin fluctuations in LSCO crystals of different doping. The data taken from [4 - 7] and normalized to the highest intensity value of each set. (right panel) (a) Representative inelastic neutron scattering data. (b) Fitted integrated intensity, normalized to the maximum value, as a function of energy transfer and applied magnetic field. Data taken on the $x=0.08$ LSCO sample shown in (c), on Thales, ILL.

- [1] Vojta, M., Adv. Phys., 58(6), 699-820 (2009).
- [2] Julien, M.-H., Physica B, 329:693–696 (2003).
- [3] Jacobsen, et al., PRL, 120(3), 037003 (2018).
- [4] Chang, J., et al., PRL, 98(7):077004 (2007).
- [5] Lake, B., et al., Science, 291(5509), 1759-1762 (2001).
- [6] Tranquada, et al., PRB, 69(17), 174507 (2004).
- [7] Rømer, A. T., et al., PRB, 87(14):144513 (2013).

PARTICIPANTS

ALTYNBAEV	Evgenii	Petersburg Nuclear Physics Institute	Gatchina	Russia	evgeniy.alt@lns.pnpi.spb.ru
BAKANGURA	Erigene	Laboratoire Léon Brillouin, CEA Saclay	Gif-sur-Yvette	France	erigene.bakangura@cea.fr
BEAUVOIS	Ketty	CEA	Grenoble	France	beauvois@ill.fr
BOEHM	Martin	Institut Laue-Langevin	Grenoble	France	boehm@ill.fr
BOUE	François	Laboratoire Léon Brillouin, CEA Saclay	Gif-sur-Yvette	France	francois.boue@cea.fr
BOUNOUA	Dalila	Laboratoire Léon Brillouin, CEA Saclay	Gif-sur-Yvette	France	dalila.bounoua@cea.fr
BRULET	Annie	Laboratoire Léon Brillouin, CEA Saclay	Gif-sur-Yvette	France	annie.brulet@cea.fr
CERETTI	Monica	Institut Charles Gerhardt	Montpellier	France	monica.ceretti@univ-montp2.fr
CHABOUESSANT	Grégory	Laboratoire Léon Brillouin, CEA Saclay	Gif-sur-Yvette	France	gregory.chaboussant@cea.fr
CHARPENTIER	Thibault	NIMBE, CEA Saclay	Gif-sur-Yvette	France	thibault.charpentier@cea.fr
CHENNEVIERE	Alexis	Organisation, LLB	Gif-sur-Yvette	France	alexis.chenneviere@cea.fr
CLEMENT	Frédéric	Laboratoire Léon Brillouin, CEA Saclay	Gif-sur-Yvette	France	frederic.clement@cea.fr
CLEMENTYEV	Evgeny	Petersburg Nuclear Physics Institute	Gatchina	Russia	EKlementev@kantiana.ru
COMBET	Jérôme	Institut Charles Sadron	Strasbourg	France	jerome.combet@ics-cnrs.unistra.fr
COUSIN	Fabrice	Laboratoire Léon Brillouin, CEA Saclay	Gif-sur-Yvette	France	fabrice.cousin@cea.fr
DA CUNHA FERREIRA	Afonso	Laboratoire Léon Brillouin, CEA Saclay	Gif-sur-Yvette	France	afonso.dcerreira@cea.fr
DAMAY	Françoise	Laboratoire Léon Brillouin, CEA Saclay	Gif-sur-Yvette	France	francoise.damay@cea.fr
DESMEDT	Arnaud	Institut des Sciences Moléculaires	Bordeaux	France	arnaud.desmedt@u-bordeaux.fr
ELIOT	Eric	Laboratoire Léon Brillouin, CEA Saclay	Gif-sur-Yvette	France	eric.eliot@cea.fr
ERMAN	Azad	Institut Chimie Matériaux Paris Est	Thiais	France	erman@icmpc.cnrs.fr
FADDA	Giulia	Laboratoire Léon Brillouin, CEA Saclay	Gif-sur-Yvette	France	giulia.fadda@cea.fr
FERDEGHINI	Filippo	ECE / LLB	Paris	France	filippo.ferdeghini@ece.fr
HIESS	Arno	European Spallation Source	Lund	Sweden	arno.hiess@esss.se
IASHINA	Ekaterina	Petersburg Nuclear Physics Institute	Gatchina	Russia	yashina@lns.pnpi.spb.ru
JESTIN	Jacques	Laboratoire Léon Brillouin, CEA Saclay	Gif-sur-Yvette	France	jacques.jestin@cea.fr
JOUAULT	Nicolas	PHENIX, Sorbonne Université	Paris	France	nicolas.jouault@upmc.fr
LE COEUR	Clémence	Organisation, LLB/ICMPE	Saclay/Thiais	France	clemence.le-coeur@cea.fr
LEMEE-CAILLEAU	Marie-Hélène	Institut Laue-Langevin	Grenoble	France	lemeec@ill.fr
LYONNARD	Sandrine	SyMMES, CEA	Grenoble	France	sandrine.lyonnard@cea.fr
MAGNETTE	Arnaud	Institut Jean Lamour	Nancy	France	arnaud.magnette@univ-lorraine.fr
MANGIN-THRO	Lucile	Organisation, ILL	Grenoble	France	mangin-thro@ill.fr
MONET	Geoffrey	Laboratoire de Physique des Solides	Orsay	France	geoffrey.monet@u-psud.fr
NATALI	Francesca	CNR-IOM / Institut Laue-Langevin	Grenoble	France	natali@ill.fr
OSTA	Oriana	Laboratoire Léon Brillouin, CEA Saclay	Gif-sur-Yvette	France	oriana.osta@cea.fr
OTT	Frédéric	Laboratoire Léon Brillouin, CEA Saclay	Gif-sur-Yvette	France	frederic.ott@cea.fr
PETIT	Sylvain	Laboratoire Léon Brillouin, CEA Saclay	Gif-sur-Yvette	France	sylvain.petit@cea.fr
PLAZANET	Marie	LIPhy, CNRS	Grenoble	France	marie.plazanet@univ-grenoble-alpes.fr
ROLS	Stéphane	Institut Laue-Langevin	Grenoble	France	rols@ill.fr
ROUSSE	Gwenaelle	Collège de France	Paris	France	Gwenaelle.Rousse@impmc.upmc.fr
SANDRE	Olivier	Laboratoire de Chimie des Polymères Organiques	Bordeaux	France	olivier.sandre@enscbp.fr
SCHOBER	Helmut	Institut Laue-Langevin	Grenoble	France	schober@ill.fr
SIBILLE	Romain	Paul Scherrer Institut	Villigen	Switzerland	romain.sibile@psi.ch
SIMON	Charles	Institut Néel	Grenoble	France	charles.simon@neel.cnrs.fr
SIMONET	Virginie	2FDN/Institut Néel	Grenoble	France	virginie.simonet@neel.cnrs.fr
SUDRE	Guillaume	IMP, EZUS, Université de Lyon	Villeurbanne	France	guillaume.sudre@univ-lyon1.fr
TRESSET	Guillaume	Laboratoire de Physique des Solides	Orsay	France	tresset@lps.u-psud.fr
TUTUEANU	Ana	Institut Laue-Langevin	Grenoble	France	tutueanu@ill.fr
ZANOTTI	Jean-Marc	Laboratoire Léon Brillouin / ILL	Grenoble	France	jean-marc.zanotti@cea.fr